ADDIS ABABA UNIVERSITY

ADDIS ABABA INSTITUTE OF TECHNOLOGY

SCHOOL OF CIVIL AND ENVIRONMENTAL ENGINEERING

RAIL CRACK ANALYSIS WITH INSPECTION AND MAINTENANCE PLAN AT TRANSITION SECTION BETWEEN BRIDGES AND EMBANKMENTS

A Thesis in Railway Civil Engineering

By Abel Beneberu

June, 2016

Addis Ababa

Advisor

Mequanent Mulugeta (M.Sc.)

A Thesis

Submitted in Partial Fulfillment of the Requirements for the Degree of Master of Science

The undersigned have examined the thesis entitled '**Rail crack analysis with inspection and maintenance plan at transition section between bridges and embankments**' presented by **Abel Beneberu**, a candidate for the degree of **Master of Science** and hereby certify that it is worthy of acceptance.

Mequanent Mulugeta (M.Sc.)		
Advisor	Signature	Date
Internal Examiner	Signature	Date
External Examiner	Signature	Date
Chair person	Signature	Date

DECLARATION

I certify that this research work titled “Rail crack analysis with inspection and maintenance plan at transition section between bridges and embankments” is my own work. The work has not been presented elsewhere for assessment and award of any degree or diploma. Where material has been used from other sources it has been properly acknowledged/ referred.

Abel Beneberu	……..	……..
Name	Signature	Date

ABSTRACT

Since railway is considered as optimal solution for the quickly growing transportation demand its design, construction and maintenance should get proper attention. In rail route design, we may need (be forced) to consider bridges and tunnels to pass obstacles (especially in countries like Ethiopia). And emphasis must be given for transition section like between bridges and embankments because when the railway route pass from embankment to bridge or vice versa the track bed stiffness (modulus) varies causing abrupt change in vertical deflection which intern leads to frequent high vertical force exerted on the track structure, that cause more frequent damage to the track systems. So, this study gives emphasis to the damage on rail occurring at this transition section (specifically from embankment to bridge or vice versa).

The study uses ABAQUS and FRANC 3D software to determine the stress that occurs on the rail at the transition section and the crack size (level of damage) respectively together with analytical equation to get some important parameters used for the analysis.

Accordingly, the analysis results shows that due to the track bed stiffness difference the crack will be 3.5 mm at the rail base and 2.5 mm at the rail head. However, in depth experiments show that the rail can serve as long as the gap due to the crack is up to 70mm. Therefore, the probability of derailment happening is small. Even if the derailment happening probability is less, as cracks can propagate with increased number of cycles, the rail should be inspected and maintained frequently. From the numerical investigation, the inspection frequency of the rail at the transition section should be four times in a year (every three month).

Finally, the conclusions of the research are presented with recommendations for further research by adding other factors that affect stiffness at transition sections.

Keywords: Track Modulus, Embankment, Bridge, Stiffness, Transition Section, Vertical Deflection, Rail Damage

ACKNOWLEDGMENTS

First and foremost I thank God for being my strength in doing this thesis work.

Then I would like to express deepest gratitude to my advisor Mequanent Mulugeta (MSc.), for his constant motivation, guidance, support, supervision and constructive suggestion throughout this thesis work.

Many thanks to my family for their patience and love and my friends for their endless collaboration. I want also to gratefully acknowledge the staff of ERC (especially the librarians). Thank you all.

Finally, I appreciate the support from Ethiopian Railway Corporation (ERC) and Addis Ababa Institute of Technology (AAiT).

TABLE OF CONTENTS

LIST OF TABLES

LIST OF FIGURES

NOTATION

ϕ	Dynamic impact factor
σ_{all}	Allowable rail bending stress
τ_{all}	Allowable rail shear stress
σ_b	Rail bending stress
τ_{max}	Maximum rail shear stress
σ_{mean}	Mean rail contact stress
σ_{th}	Rail temperature stress
σ_{ult}	Ultimate tensile strength of rail
σ_y	Rail yield stress
FEA	Finite Element Analysis
AREMA	American Railway Engineering and Maintenance-of-Way Association
FEM	Finite Element Modeling
CAE	Complete ABAQUS Environment
FRANC3D	Fracture Analysis 3 Dimensional
R	Shear resistance
2D	Two Dimensional
3D	Three Dimensional
D-P/DP	Drucker-Prager
k	Ratio of the yield stress
ρ	Density
g	Acceleration due to gravity
h	Depth
ν	Poison's ratio
E	Elastic modulus

ψ	Dilation angle
GB	Chinese Railway manual
U	Track modulus
P	The vertical track load;
Y	Deflection
I	Moment of inertia of the rail cross section.
CWR	Continuously Welded Rail
σμ	Mean Hertz stress (q_{mean})
K	Flow stress ratio
P^D	Design wheel load
Ps	Static wheel load
MGT	Million Gross Tone's
SIF	Stress Intensity Factor
g	Acceleration due to gravity
h	Depth
P_c	Confining pressure
ν	Poison's ratio
E	Elastic modulus
ψ	Dilation angle

1. INTRODUCTION

1.1. Background

In the contemporary world the need for fast, environmentally friendly and energy saving transportation system is highly increasing. And now a days Railway transportation is being optimal solution for the quickly growing transportation demand.

Currently railway construction in our country is also a main task to develop or to strengthen the transportation sector and to meet the country's five year National Growth and Transformation plan. According to this plan besides to other types of constructions, railway is one of the main construction activities getting major emphasis in the transportation sector. Therefore, the government launched many railway lines in the capital city Addis Ababa and on different locations of the country.

In the design and construction of a Railway line, especially in countries like Ethiopia with mountainous topography, as the train cannot climb steep slope, the route may pass through different landscape like over an obstacle (which may be a valley, under pass road, a river and soon) by constructing a bridge or through a mountain by tunneling. When the railway route pass from embankment to bridge or vice versa and from tunnel to embankment or vice versa the track bed stiffness varies. When stiffness difference occur, in addition to the vertical deflection more frequent high longitudinal force is exerted on the track structure, which cause more frequent damage to the track systems. Consequently, attention should be given to the design, construction and maintenance of the Railway infrastructure.

The transition between embankment (ballasted) and slab (ballastless) track is a weak point in heavy haul and high-speed railways as shown in figure below. Strong vibrations occur in the train, railway track components, and support structures when the trains transition between ballasted and concrete slab tracks. These vibrations may cause an amplified load on the supporting structures, but the response of the slab track is deferent from that of the embankment. On the embankment section it may cause mud pumping of the ballast, swinging, or hanging sleepers, ballast breakdown, rail battering, concrete sleeper cracking and differential settlement, and loss of surface and gauge. These problems then directly affect the running stability of the trains and may even create the potential for derailment.

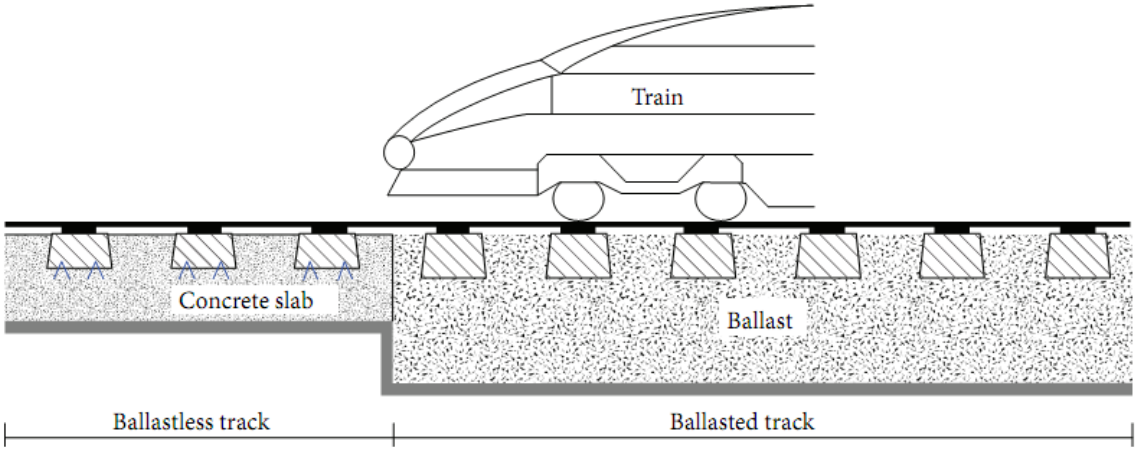

Figure 1.1 a schematic layout of the railway ballastless-ballasted transition (X. Lei and L. Mao, 2004).

Derailments results from one or more of a number of distinct causes; these may be classified as:

- The primary mechanical failure of a track component (for example broken rails, gauge spread due to sleeper (tie) failure)
- A fault in the geometry of the track components or the running gear that results in a quasi-static failure in running (for example rail climbing due to excessive wear of wheels or rails, earthworks slip)
- A dynamic effect of the track-vehicle interaction (for example extreme hunting, vertical bounce, track shift under a train, excessive speed)
- Improper operation of points, or improper observance of signals protecting them (signal errors)
- As a secondary event following collision with other trains, road vehicles, or other obstructions (level crossing collisions, obstructions on the line)
- Train handling (snatches due to sudden traction or braking forces)

  Add other countries railway accidents due to derailments

From the above causes of derailments that causes most of the railway accidents one of the major reasons is broken rails that mostly advance from rail crack. So in order to minimize railway accidents attention should be given to rail crack or rail damage that can happen due to different factors like track stiffness difference, rail fatigue, temperature effect and soon. From these different factors this research give special attention to the rail damage occurring due to the track stiffness difference at transition locations.

Although we don't have experience and past data, from other countries experience most derailments happen due to rail damage. For example in Australia as shown in figure 1.2 derailments still happened regardless the effort of railway operators and safety regulators to improve rail safety by providing appropriate safety legislation and better vehicles.

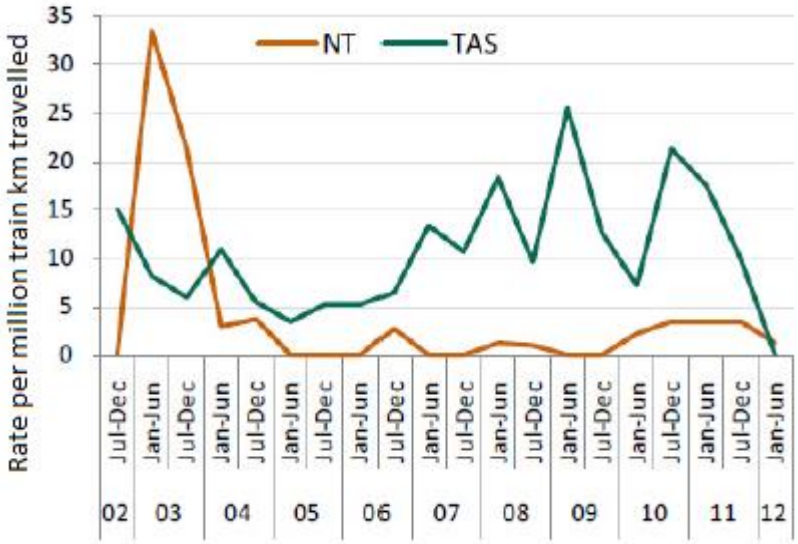

Figure 1.2 Rate of Australian running line derailments per million km (Australian Transport Safety Bureau, (2012))

Table below also shows a list of the type of derailments attributed to rail defects from 1992 to 1995 in USA. The breakdown of cost associated with the derailments also is listed.

Table 1.1 Rail Derailments, 1992–1995 in US

Cause	**1992**	**1993**	**1994**	**1995**	**Total**	**Total Costs**
Bolt Hole crack	3	7	8	9	27	$5,469,179
Broken Weld	3	3	4	7	17	$3,762,576
Detail Fracture	15	12	17	14	58	$14,856,282
Head Web	25	31	25	30	111	$7,618,514
HSH	7	8	5	6	26	$1,341,679
Broken Bars	9	6	9	6	30	$3,607,822
TD	37	46	32	44	159	$21,366,484
VSH	24	35	40	27	126	$12,936,719
Totals	**123**	**148**	**140**	**143**	**554**	**$70,959,255**

(Data is from U.S. Federal Railroad Administration "Accident/Incident Bulletin")

Notes: Broken base and broken bolt derailments are not included, since they cannot be detected by ultra-sonic detector cars.

HSH – Horizontal Split Head TD – Transverse Defect VSH – Vertical Split Head

When stiffness difference occur, in addition to the vertical deflection more frequent high longitudinal force is exerted on the track structure, which cause more frequent damage to the track systems such as wheel-rail plastic flow, cracks on rail and substructure, and wheel-rail rolling contact fatigue defects. Therefore the wheel/rail contact problems associated to rail support stiffness difference need to be studied in detail.

The problems associated with the transition section are investigated by some researchers. Some studies focused on modelling and simulating the vehicle-track interaction at transition sections, and the principle vibration source is thought to be the abrupt change in track stiffness during the transition due to the concrete slab track stiffness being far larger than that of the ballast track. But most literatures don't specify the severe damage which occur on the rails by this stiffness difference at transition locations. Other studies also investigated remedies to effectively address the resultant problems. But for already constructed routes we need to device appropriate maintenance methods and schedules.

The thesis explores the impact of the variation of the rail support stiffness difference on the rail damage and intern the rail damage led us to the contribution of this factor to the derailments and other series accidents. Based on the research output, a better planning of maintenance schedule of the railway system will be forthcoming to maximize the service life of the train and tracks and minimize the railway accidents.

1.2. Statement of the problem

The track stiffness experienced by a train will vary along the track. Sometimes the stiffness variation may be very large within a short distance especially at transition from an embankment to a bridge. Quite often, due to the substructure, there are large changes of the track stiffness within short distances. The transition area from an embankment to a bridge is a place where large track settlement may occur. The variations of track stiffness will induce variations in the wheel/rail contact force. This will intensify track degradation such as increased wear, fatigue, track settlement due to permanent deformation of the ballast and the substructure, and so on. As soon as the track geometry starts to deteriorate, the variations of the wheel/rail interaction forces will increase, and the rail deterioration rate increases. Therefore, it is important to give special attention to this transition section and consider appropriate inspection and maintenance.

1.3. Significance of the Study

In our country Ethiopia, it is known that the railway industry is emerging and moving forward by the ongoing 5000kms rail route construction in the national grid and more than 34kms Light Rail Transit (LRT) in the capital city Addis Ababa. Consequently, in these all railway lines there has been many overpass bridges and tunnels, which needs special attention since transition locations are weak due to the varying stiffness difference. So this research tries to assess the damage on rails occurring due to stiffness difference of tracks at transition from embankment to bridge or vice versa and also tries to provide different methods of maintenance and inspection.

1.4. Research objectives

1.4.1. General objective

The general objective of the study is to analyze the damage occurring on rails due to a stiffness difference happening at transition between embankment and bridge and to device a better maintenance and inspection plan which ultimately try to minimize the accidents and failures which the railway transportation sector faced.

1.4.2. Specific Objectives

- To find the stress increment between the ballast (embankment) and slab (bridge) sections that causes the rail damage at this transition zone,
- To determine the damages on the rails of the track structure at transition from bridge to embankments or the vice versa,
- To suggest an optimal maintenance and inspection schedule which should be followed to minimize the effect of the expected damage on rail at transition points.

1.5. Scope and Limitations

The scope of the study is to determine the stress on the rail and investigate the corresponding deflection and damage occurring on the rail component due to rail supporting track structures stiffness difference at transition location and based on the damage expected the study tries to set recommended maintenance schedule.

Some of the limitations which occur during the study includes:

- Since the model is huge, the analysis required computers with higher processer capacity and the time for analyzing the model was also long,
- Again because of the largeness of the model the mesh size considered for 2D transition section analysis is courser, and
- The rail geometry do not perfectly match the actual rail profile because of the difficulty to run a 3D model that seems near to the actual track model because of the limitation of the model analyzing computer capacity but since the moment of inertia difference between the simplified and the actual rail is less than 2% the results will not be affected mach.

1.6. Methodology

Literatures regarding rail damage and transition section are thoroughly studied and reviewed. Technical papers, manuals, journals and publications regarding the effect of track modulus difference on the rail were reviewed. The data and data sources are from Chinese Railway manual (GB) which the Ethiopian Railways are designed from, American Railway Engineering and Maintenance-of-Way Association (AREMA) manual and other acknowledged publications.

First two dimensional Finite element modeling and analysis together with some mathematical evaluations of different parameters is done for the whole transition section (which includes both the bridge and the embankment sections) to determine the stress on the rail at this transition zone.

Next, a three dimensional 60kg/m rail which is subjected to an amplified stress (because of sudden stress variation) is modeled to determine the expected crack size which enable us to recommend the frequency of rail inspection and maintenance at transition section.

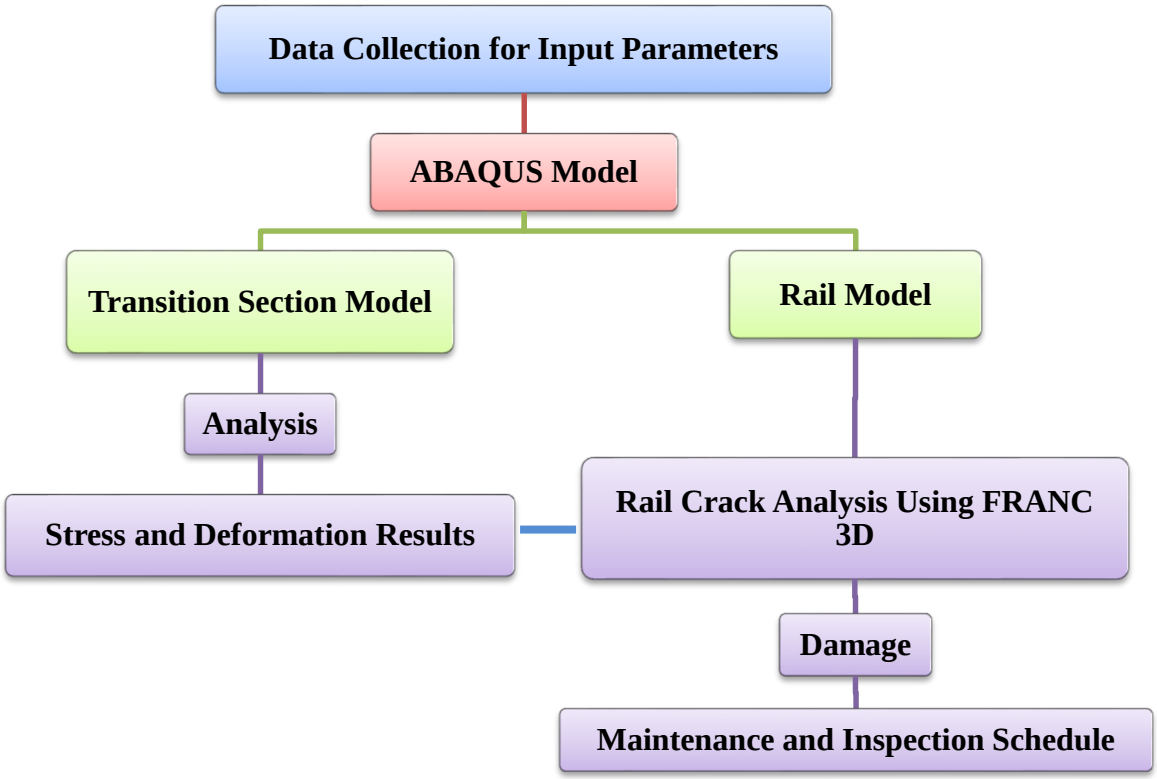

Figure 1.3 Overall Thesis Flow Diagram

1.7. Thesis Outline

This thesis is divided into five chapters. A brief outline of this thesis is given below:

Chapter 1 is the introductory as stated above which contains the general background, statement of the problem, objectives of the research, methodology and structure of the thesis.

Chapter 2 is the literature review begins with a general description of the railway system discussing about the embankment and the bridge location separately. This is followed by reviewing the wheel-rail contact characteristics of the track system in general. Following the wheel-rail contact concept, details about rail loads and stresses is reviewed which includes all the vertical, lateral and transversal loads and their stress effect on the rail. The next topic reviewed is damage mechanisms on wheel-rail contact due to the applied loads and expected stresses. Then finally since the rail is needed to serve its function safely in its design period it needs maintenance and inspection track maintenance concept is discussed.

Chapter 3 is finite element modeling and analysis and holds three concepts; an introduction, transition zone two-dimensional ABAQUS model and separate three dimensional rail model for crack analysis. The analysis begins by giving general introduction to finite element modeling and analysis. Following the introduction a 2D model of the transition section and analysis to get the stress increment has been performed which includes geometry and material properties, assembly and interaction, loading and boundary conditions, meshing of track components. Finally a 3D rail modeling and analysis is presented which later can be an input for crack analysis in FRANC3D.

Chapters 4 present analysis results and discussions based on the finite element models and analysis done in the third chapter. The stress and deformation results obtained at the transition zone are presented and used for the detail crack analysis on the rail using FRANC3D software. And at last relaying on the crack analysis output the frequency of rail inspection recommendations are presented.

Last chapter, **Chapter 5** summarizes the main findings of this research study; conclusions have been made based on the result of the FEM analysis. Finally, several recommendations are made for further research. This chapter is followed by a list of references.

2. LITERATURE REVIEW

2.1. Description of the railway system

In railway systems, the main functions of the track are guiding the train, carrying the loads and distribute the loads to a larger area. Tracks can be divided into two types as ballasted on embankment section and non-ballasted (slab) tracks on bridge section. The track superstructure components can also differ significantly with regards to their geometrical, material and physical properties (Andersson E, Berg M and Stichel S, (2007)).

The structure of a track in embankment locations includes some components such as rails, railpad/fastening, sleepers, ballast, subballast and subgrade. Two subsystems of a ballasted track can be distinguished: the superstructure (rails, sleepers, ballast and sub-ballast) and the subgrade (composed of a formation layer and the base). Plastic or rubber rail pads are usually located between the sleepers and the rails. The sleepers are embedded in a ballast layer which in turn is resting on subballast and subgrade.

The railpad's, (J. Maes, H. Sol, and P. Guillaume, (2006)), applications are to protect sleepers from wear and damage due to the high impact loading, and also to reduce the high frequency vibration and the role of fastening is to fix the rail in position and to prevent the rail from rolling over when it is affected by lateral forces. The sleeper, (G. Zi, S. Y. Jang, S.C. Yang, H.S. Lee, E. Kim, (2012)), also plays an important role in track dynamics as well as railpad. In addition to electrical insulation benefit, this component allows the loads acting on the rail to transfer down to ballast. Ballast, (W. M. Zhai, (2004)), is the selected material placed on top of the track subgrade to support the track structure against vertical, lateral, and longitudinal forces from the trains. The sleepers, to which the rails are fastened, are embedded in the ballast, which is tightly compacted or tamped around the sleepers to keep the track precisely levelled and aligned. The standard depth of ballast is 0.3-0.35 meters. Below the ballast a layer of sub-ballast is placed. The sub-ballast is material chosen as a transition layer between the ballast and the subgrade to prevent the mutual penetration or intermixing of the subgrade and the ballast and to reduce frost penetration. Subgrade is the layer of material on which the ballast and sub-ballast layers rest. The subgrade is a very important component in the track structure and has been the cause of track failure and development of poor track quality (Li and Selig,

1995). Unfortunately, in existing track, the subgrade is not involved in the maintenance operation and little can be done to alter its characteristics.

The structure of a track in bridge locations includes some components such as sleepers, Slab Bridge, abutment and subgrade. In bridges, the ballast bed is omitted and replaced with concrete slabs which takes loads from the sleepers and transfer it to the adjacent abutment structures. Abutments are vertical structures which are responsible to transfer loads from Slab Bridge to the subgrade on overpass sections and it retain the embankment laterally.

From the dynamic point of view, each of the components above has significant influences on the operation of the railway system. Therefore study of the track system should account for the effects of these track components.

2.1.1. Railway Track Transitions

Railway track transition zone is a zone where track stiffness changes abruptly (Dingqing Li and David Davis (2005)). This change occurs where the slab track connects to a conventional ballasted track, at the abutments of open-deck bridges, at the beginnings and ends of tunnels, at road and railway level crossings, and at locations where rigid culverts are placed close to the bottom of sleepers. There are three categories of track transitions. The first is elastic stiffness change, for example, going from an earth support to a bridge support for the track. The second is change in plastic deformation under repeated wheel loading caused by local changes in subgrade soil strength or dynamic load variation. The third is change in maintenance effort, for example, stopping tamping at grade crossings. These categories are interrelated because maintenance change can cause change in elastic and plastic properties. These transitions all produce dynamic load which, when excessive, result in damage to the track structure and create a need for more maintenance.

2.1.1.1. Vertical track stiffness and Track modulus

The terms “vertical track stiffness” and “track modulus” are related through the bending stiffness of the rail (Selig, E. T., and Li, D. (1994)). Thus, if either is known, the other can be calculated.

Table 2.1 Track stiffness verses Track modulus

Track stiffness	Track modulus
Track stiffness refers to the rails It is ➢ The elastic rail deflection that takes place under a wheel loading. ➢ The ratio of the load applied to the rail to vertical rail deflection.	Track modulus refers to the track It is ➢ The stiffness of the spring k per unit length of track. ➢ A measure of the vertical stiffness of the track foundation.

For a railroad track, "track modulus" is often used as a measure of vertical stiffness of the rail foundation and is defined as the supporting force per unit length of rail per unit vertical deflection under a vertical load, as determined by the following equation (Selig and Waters 1994):

$$u = \frac{K^{\frac{4}{3}}}{(64EI)^{\frac{1}{3}}} \text{ ---------- 2.1}$$

$$k = \frac{P}{Y} \text{ ---------- 2.2}$$

Where

- u=track modulus (in the unit of N/mm/mm or lbs. /in. /in.);
- P= the vertical track load;
- Y=deflection;
- E=Young's modulus of the rail; and
- I=moment of inertia of the rail cross section.

Low track modulus is often associated with weak subgrade support, whereas a high track modulus can accelerate undesirable dynamic vehicle/track interaction. Generally, track modulus reflect stiffness characteristics of the track and subgrade layers.

Therefore, one important track problem which needs special attention is the severe change in vertical stiffness (Y. S. Kang, S.C. Yang, H.S. Lee, E. Kim, (2006)). In the transition zone, the vertical level of running wheel changes due to variations in track

vertical stiffness. This change in elevation causes vertical acceleration imposition on running coach. Variable accelerations cause vertical dynamic load to change. The level of variations depends on the vertical displacement of rail in both sides of the transition zone, train speed, track modulus variations, and other factors. The sudden change in track vertical stiffness leads to uneven deflection, which causes abrupt change in the vertical level of the vehicle's wheels. This change in elevation will excite the train component, i.e., the wheels, bogies, and coach, which in turn leads to vertical train–track interaction forces that are dynamically amplified in the transition zone.

2.2. Rail Loads and Stresses at Transition Section

All major rail defects require some form of stress to initiate and develop. Consequently, before rail defects can be discussed in any detail, it is necessary to have some understanding on the loads that are applied to the rails and result stresses.

2.2.1. Rail Loads at the Transition Zones

Transition zones are usually associated with track geometry deterioration that requires frequent maintenance. This change of stiffness causes increased dynamic forces, which depends on the speed, the stiffness ratio, the damping properties and the transition length.

Transition zones can usually be found near bridges, abutments and tunnels. When a train enters a bridge, the change of the stiffness on the transition zone between the plain track and the bridge (on plain track i.e. $E \approx 1*10^8$, on the bridge $E \approx 35*10^{9)}$ often causes problems. The observed problems in the transition zone can include

- Ballast penetration into the subgrade,
- Hanging sleepers (i.e. voids forming underneath the sleepers),
- Permanent rail deformation,
- Worn track components
- Cracking of the sleepers (and/or slab track) and
- Loss of gauge

Generally, the wheel loads acting on the rail can be divided into three components, which are vertical, lateral and longitudinal forces.

The vertical force results from the weight of the wheel and the car bodies. The lateral force is generated due to the movement of the wheel set on the rail, and is especially high on the curved track. The longitudinal force is the traction force which is produced by the locomotives.

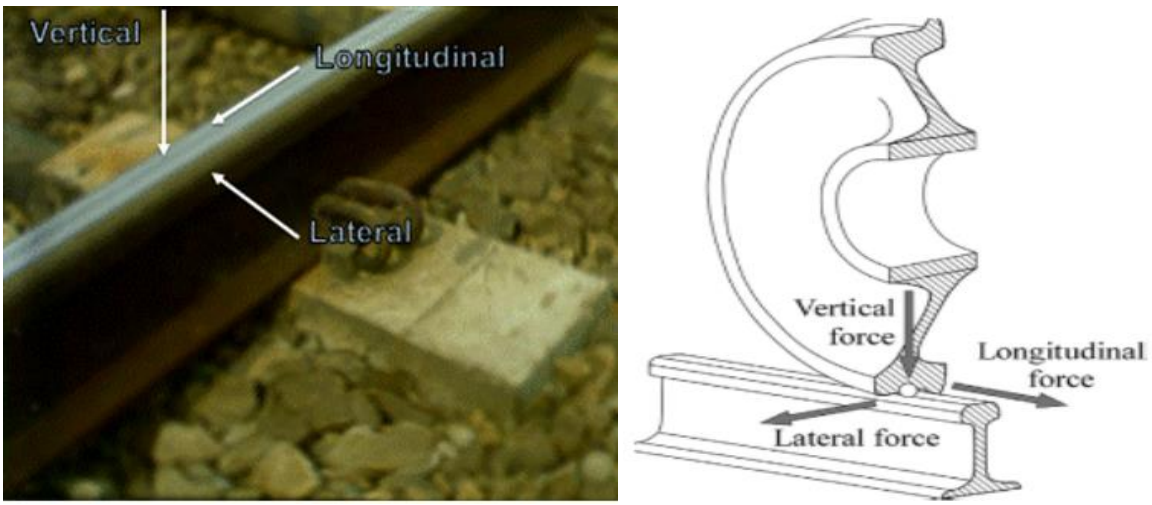

Figure 2.1 contact forces on the rail (U. Zerbst, (2009))

For simplified analysis some loads can be considered static, constant in direction and magnitude. These loads are typical dead loads or used in analyzing a member at a given moment in time. Dynamic loading is typically the true loading scenario, however is greatly more difficult to model. To describe dynamic loading perfectly every imperfection (like track irregularity) in the rail structure must be known. Similarly, in transition section an amplified dynamic load exist which cause severe deterioration on the rail structure.

2.2.2. Stresses on the Rail Structure

Rails are supported by ballast, crossties, and assembly fittings to transmit in case of ballasted tracks and by slab and abutment in case of slab track and distribute wheel loads to the subgrade. The structural support restrains the track from movement in the lateral, longitudinal, and vertical directions under dynamic wheel loads and thermal stresses (Timoshenko, S., Langer, B., (1932)). Moreover, the quality of the track structure is defined by rail size and support characteristics. The flexural behavior of a rail in track under passing wheel loads can be accurately assessed using an analysis of the rail as a uniform beam on elastic foundation. Rail stresses, however, are also dependent on local

variations in support stiffness and the ability of the structure to transfer applied loads to the supports. In addition, heavy trains operating at high speeds can initiate a cycle of accelerated degradation of geometry that feeds back through vehicle response to track irregularities to cause even larger demands on the track.

P. Paris and F. Erdogan (1963), internal defects develop and grow in rail due to the repeated passage of trains, i.e. metal fatigue. Fatigue and fracture analyses are applied to calculate the growth rate of the defects and to predict the critical conditions when the defects become large enough to cause a broken rail.

David Y. Jeong, A. Benjamin Perlman, (2011), Operational factors determine the magnitude of the applied wheel loads. These operational factors include the characteristics of different car types, train speed and track condition. Structural factors are shown to comprise the rail and the support conditions (i.e. foundation and ties). The response of the track structure to the applied wheel loads is then calculated in terms of rail stresses.

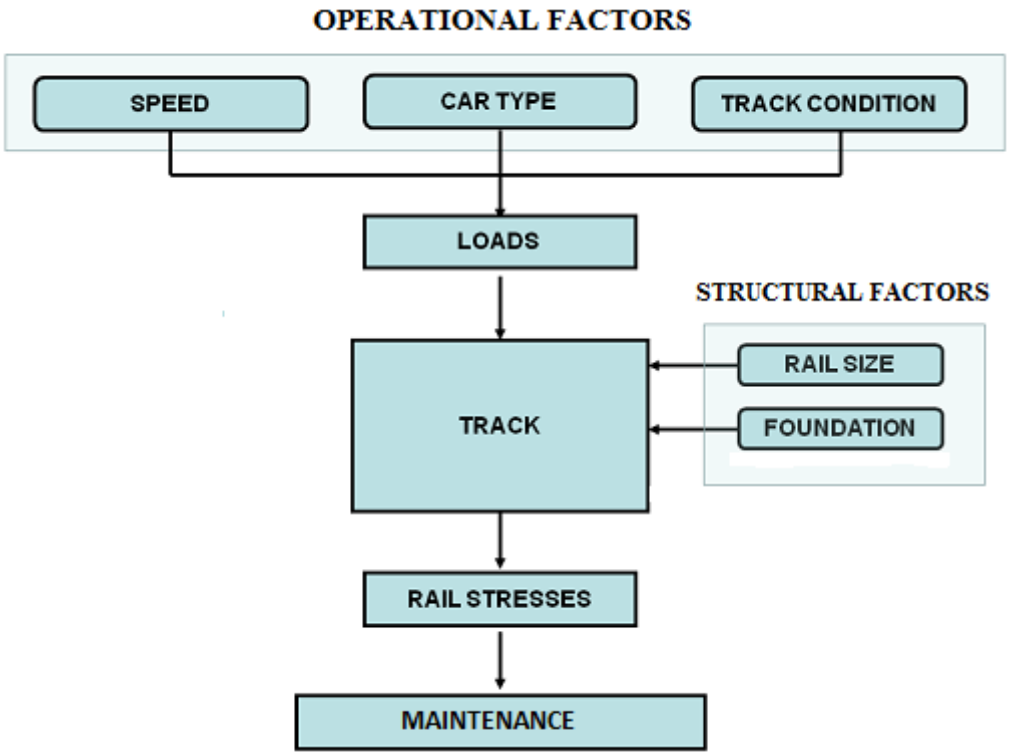

Figure 2.2 Flow diagram for estimating track capacity limit (David Y. Jeong, A. Benjamin Perlman, (2011))

To evaluate the load-bearing capacity of rail, a criterion is assumed to define a stress state beyond which represents catastrophic failure of the rail.

The total stresses developed on the rail are the sum of (Esveld, 2001):

- Hertz stresses (at the wheel-rail contact)
- Stresses resulting from bending of the rail
- Stresses resulting from thermal effects
- Plastic stresses, remaining on the rail after the removal of external loads
- Stresses due to track modulus difference.

With the exception of the last category, all others will be calculated on the assumption of an elastic behavior.

2.2.2.1. Stresses at wheel-rail contact

According to Herz's the most important assumptions on wheel-rail contact are:

- The two contact bodies are linearly elastic materials.
- The elastic displacement and the stresses become unnoticeable far from the contact area.
- The radii of the bodies at the contact must be larger than the contact size (semi-infinite bodies are assumed).
- The surfaces are smooth.
- The contact surface is elliptical and the contact pressure distribution is semi-ellipsoid.

Since the contact area is elliptical, the contact pressure is performed as the following equation:

$$Pz(x,y) = Po\sqrt{1-\frac{x^2}{a^2}-\frac{y^2}{b^2}} \quad \text{With} \begin{cases} -a \leq x \leq a \\ -b \leq y \leq b \end{cases} \text{----------2.3}$$

In which a and b are the semi-axes on the longitudinal and lateral directions.

The following two-dimensional simplified approximation can also give satisfactory results (Eisenmann's theory). Assuming that all radii of curvature (with the exception of the wheel radius R (in mm)) are infinite and that the wheel load Q (in kN) is uniformly

distributed, the mean Hertz stress or mean stress (q_{mean}) is derived according to the Eisenmann analysis from the following relation,

$$\sigma_\mu = \sqrt{\frac{\pi QE}{64Rb(1-\upsilon^2)}} \quad \text{----------2.4}$$

Where:

- Q [kN] is vertical wheel load,
- R [mm] is radius,
- σμ or q_{mean} [N/mm2] is mean Hertz stress,
- E [KPa] is modulus of elasticity,
- υ is Poisson's Ratio,
- b [mm] is semi-axes in lateral directions

Maximum shear stress in the rail head

The stress state in the rail head can be approximated sufficiently by using the Boussinesq half space theory. So the Eisenmann's simplified approximation gives the shear stress distribution of fig. 2.11b and the maximum value:

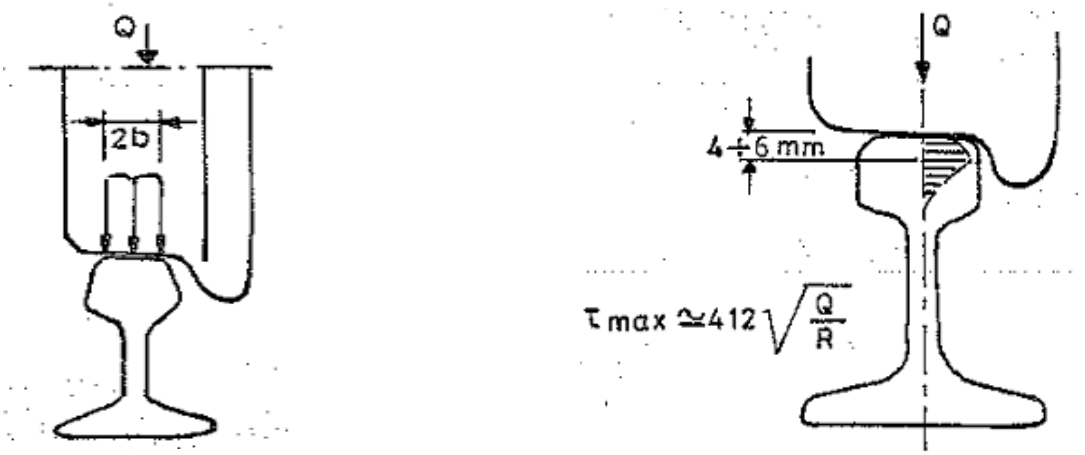

(a) (b)

Fig 2.3 (a) wheel-rail contact stresses (b) shear stress at the wheel-rail contact (Esveld, 2001)

$$\tau_{max} \cong 412\sqrt{\frac{Q}{R}} \quad \text{----------2.5}$$

Maximum shear stress occurs across the rail. Longitudinally the shear stress decreases with the occurrence of bending stresses. The simplified calculation model can be used to

calculate that the maximum shear stress according to Hertz occurs at a depth of 4-6 mm from the rolling surface in the rail head.

Permissible shear stress

On the basis of the von Mises yield criterion, the permissible shear stress may be expressed as:

$$\tau = \frac{\sigma}{\sqrt{3}} \quad \text{----------2.6}$$

- In which τ is the permissible tensile stress. On account of the fatigue nature of the load, the permissible tensile stress should, according to test, be fixed at 50% of the tensile strength σ of rail steel, thus resulting in:

$$\tau \approx 0.3\ \sigma_t \text{----------2.7}$$

2.2.2.2. Stresses resulting from bending of the rail

Esveld, 2001, bending of the rails can occur because of a range of factors, including:

- ✓ The applied vertical wheel loads, which cause the rail to bend vertically between the sleeper supports. This leads to tensile longitudinal stresses in the rail foot. The vertical loads also cause the rail head to bend vertically on the web support.
- ✓ The applied lateral wheel loads, which cause the rail head to move laterally relative to the foot. This leads to tensile vertical stresses in the rail web.
- ✓ The vertical loads that are applied at some distance from the rail center line leads to torsion of the rail, which can also cause additional tensile vertical stresses in the rail web and tensile longitudinal stresses on the fishing surface.

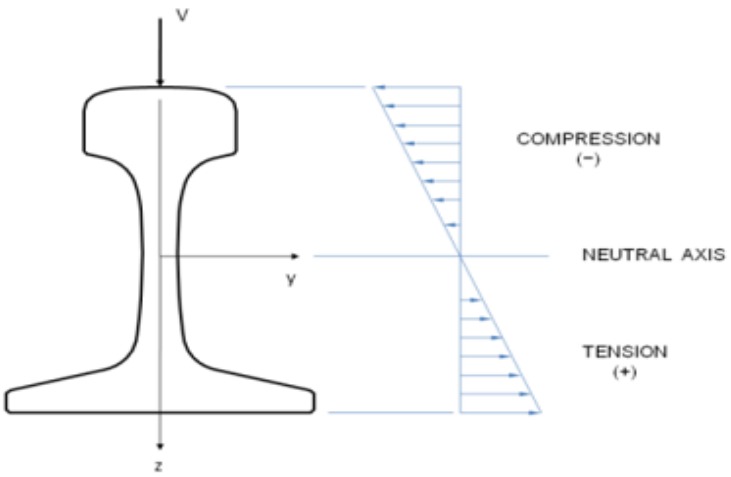

Figure 2.4 Rail bending stress due to vertical load (Timoshenko and Langer, 1932)

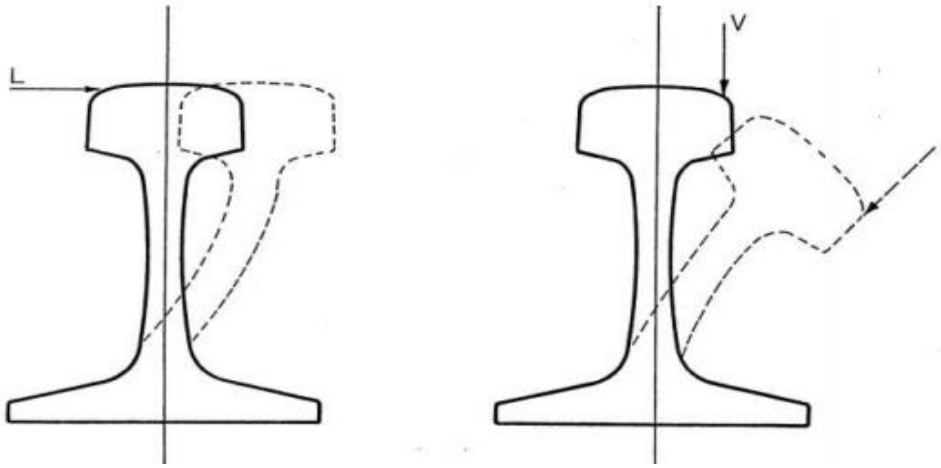

Figure 2.5 Rail Deflection from Lateral and Eccentric Vertical Loads (Timoshenko and Langer, 1932)

The maximum rail stress cannot exceed a limiting value, such as the yield strength of the rail steel. Under train-induced loading, the maximum tensile stress occurs at the field-side corner of the rail base as shown in figure 2.5. Assuming such a criterion presumes that yielding of the extreme fibers in the rail base results in catastrophic rail failure.

Since rail loads are cyclic, an evaluation of rail structural integrity based on fatigue crack growth is considered as a reasonable alternative failure criterion. For this purpose, a particular defect, called a detail fracture, is assumed to be present in the upper gage corner of the rail head because it is most common transverse rail head defect found in continuous welded rail (CWR).

2.2.2.2.1. Bending stresses of the rail on the ballast

Assuming the rail is simulated by a continuous beam on elastic supports, the general equation of mechanics:

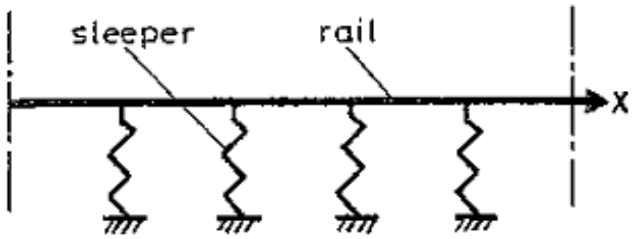

Figure 2.6 rail on elastic support (Esveld, 2001)

The bending stress of the rail on the ballast will be:

$$\sigma_b = \frac{Q(h_r - Z)}{4\gamma_r I_r} e^{-\gamma_r x}(\sin\gamma_r x - \cos\gamma_r x) \quad \text{----------2.8}$$

Where: Q = the load per wheel

Ir = the rail moment of inertia in the vertical direction

Hr = the distance between rolling line and neutral axis of the rail

K = the track index = r/z, where r is the theoretically uniformly distributed load of the wheel on rail and z is the rail vertical settlement

$$\gamma_r = \sqrt[4]{\frac{k}{4EIr}} \quad \text{----------2.9}$$

2.2.2.2.2. Bending stresses of the rail head on the rail web

The rail head is simulated as a beam laying on an elastic sub-base. The resulting stresses confirm to the analytical expression,

$$\sigma_b = \frac{Q(h_c - Z)}{4\gamma_c I_c} e^{-\gamma_c x}(\sin\gamma_c x - \cos\gamma_c x) \text{----------2.10}$$

Where: Ic = the moment of inertia of the rail head, $\gamma_c = \sqrt[4]{\frac{Ic}{4}}$ ----------2.11

hc = the distance between rolling line and neutral axis of the rail head

2.2.2.3. Stresses caused by thermal effects

These stresses occur in long welded or continuously welded rails because of the longitudinal thermal expansion and contraction that occurs as the actual rail temperature increases above or reduces below the stress free temperature at which the rails are field welded. These are derived from the well-known equation:

$$\sigma_{th} = \alpha E \Delta\theta \text{----------2.13}$$

Where: α: the rail thermal expansion coefficient

Δθ: the temperature difference

2.2.2.4. Plastic stresses

Up to present, no satisfactory elasto-plastic analysis for the calculation of plastic stresses within rails has been conducted. A fundamental reason for this has been the difficulty in simulating limit conditions between the rail and the sleeper and in determining numerical values for the parameters of the elasto-plastic calculation.

Measurements have yielded a plastic stress distribution as shown below.

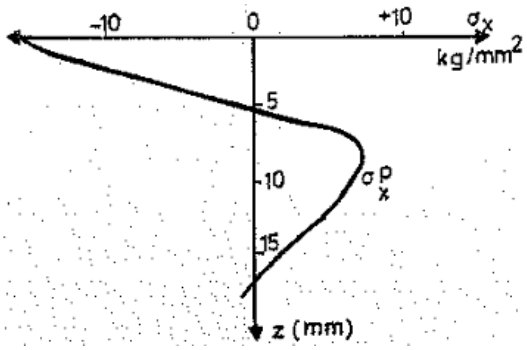

Figure 2.7 Longitudinal plastic stresses at the plane of symmetry of the rail (Esveld, 2001)

2.2.2.5. Stresses due to track modulus difference.

Variation in rail supporting foundation stiffness (track modulus) also increases the stress happening on the rail structure. Track modulus difference occurs in transition sections. (Singh, 2003) indicated that the high track stiffness on bridges and abrupt stiffness change might have caused or contributed to track geometry degradation and concrete tie cracking. He further investigate the effect of these track stiffness conditions by vehicle/track dynamic simulation analysis done using NUCARS New and Untried Car Analytic Regime Simulation, a software developed by TTCI for simulating railroad vehicle/track dynamic track interaction. At typical freight train operation speeds, the theoretical modeling has shown that, even without any initial differential track settlement, a large track stiffness change alone would lead to marginally higher 6% dynamic load variation between the approach and bridge sections**.** More importantly, it would lead to redistribution of rail-tie interaction forces over the approach and bridge areas, i.e., much higher rail-tie interaction forces on the bridge than in the approach. If a differential settlement due to geometry degradation is also present, then both dynamic wheel loads and rail-tie interaction forces will become very significant in the approach and bridge areas.

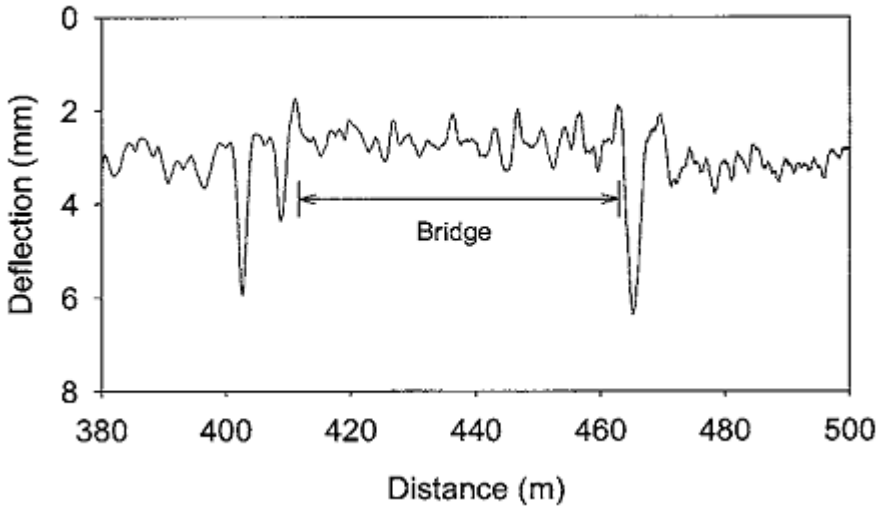

Figure 2.8 Loaded track deflection profile measured under a typical wheel load (Dingqing Li and David Davis 2005)

Also according to Y.S. Kang, S.C. Yang and H.S. Lee, contact forces, rail acceleration and vertical deflection abruptly change in transition of slab track and ballasted track. A change in the track vertical stiffness and track irregularities lead to the wheel and track to experience impact load. Dynamic impacts on wheel and rail may develop track irregularity growth. The contact forces and rail acceleration are more increased than transition without irregularity.

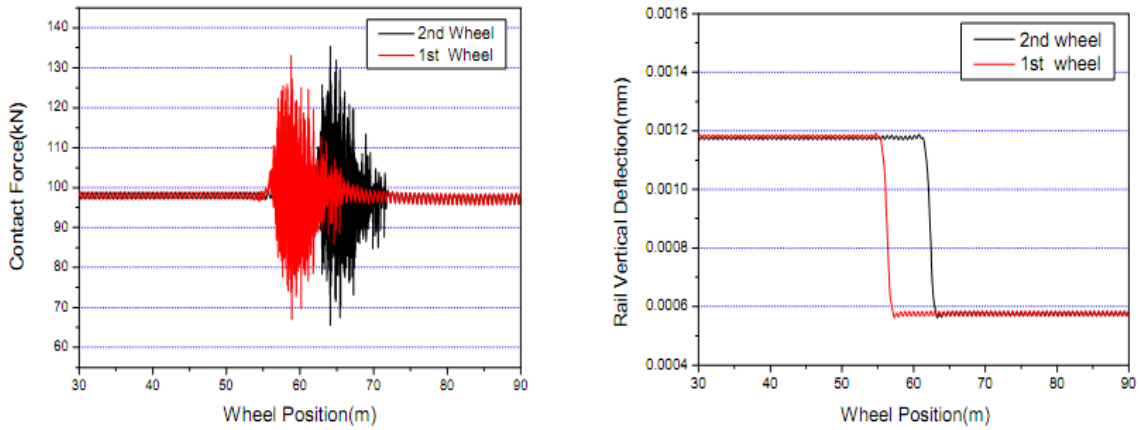

(a) Contact Force (b) Rail Vertical Deflection

Figure 2.9 Dynamic behaviors of transition

All the above stresses will play important role in the rail life cycle, particularly if a rolling contact fatigue (RCF) crack is allowed to become too large. This will also be critical if more than one stress happen at the same time.

2.3. Damage mechanisms on wheel-rail contact

The wheel-rail profile change and/or breakdown largely contribute to the maintenance or renewal cost for the track. Depending on the wheel impact load, wheel-rail materials may respond in different ways which result in various damage occurrences. The damage modes in wheel-rail contact can be classified into:

- Plastic deformation
- Wear
- Rolling contact fatigue

Plastic deformation

Xiaoi Shi, 2009, Plastic deformation is the non-reversible material disfigurement, which is predominantly caused by high traction load. During operational life, rails typically experience millions of load cycles from the passage of train wheels. The response of material subjected to repeated loading is governed by stress, strain, wear and temperature change.

Wear

Wear is defined as the displacement or the loss of material on the contact surface. This phenomenon happens whenever the contact surfaces come into sliding on each other. According to (Wilson, L., 2006), wear was sorted out into “severe wear” and “mild wear”. Mild wear prevailed on the rail head, while severe wear predominated on the rail gauge. In comparison to the original surface, a smoother surface will be generated if mild wear happens, but a rougher surface will be produced in case of severe wear. Experiments from laboratory also showed that at higher sliding speeds, a higher wear coefficient was produced, and the wear changed from mild wear to severe wear. The wear rate significantly reduce with the presence of water lubrication, but temperature in contrast increase wear effect.

Rolling contact fatigue

In general, rail cracks are categorized into two groups which are subsurface-initiated and surface-initiated cracks (U. Zerbst, (2009)). The cracks initially develop at the subsurface often result from the metallurgical defects. In addition, the travelling intensity (number of load cycles) and the axle load are two other main reasons causing surface-initiated crack.

2.3.1. Factors Influencing Rail Degradation

The identified factors responsible for rail degradation are illustrated using a cause and effect diagram in figure below and can be described as follows:

According to (IHHA, 2001) factors responsible for rail degradation are Axle load, Speed, Tamping, Rail-Wheel, Interaction, Track Curvature, Inspection Interval, Super elevation, Operational Environment (especially Water (Bower and Johnson, 1991)), Rail Hardening, Rail Welding.

According to (Esveld, 2001) additional factors are stated like Million Gross Tonnes (MGT), Rail-Wheel Material Type, Inclusion of Residual Stress, Rail Size, Track Construction and Condition of Assets and Ballast Cleaning (Lichtberger, 2005), Characteristics of the Bogie Type (Larsson, 2004) Grinding Frequency (Rippeth, 1996), Lubrication Frequency: (Diamond and Wolf, 2002).

In addition to the above factors Age of Rails, Traffic Density, Track Elevation, Formation of Blowholes and Track Accessibility can also be mentioned as a factor for rail degradation

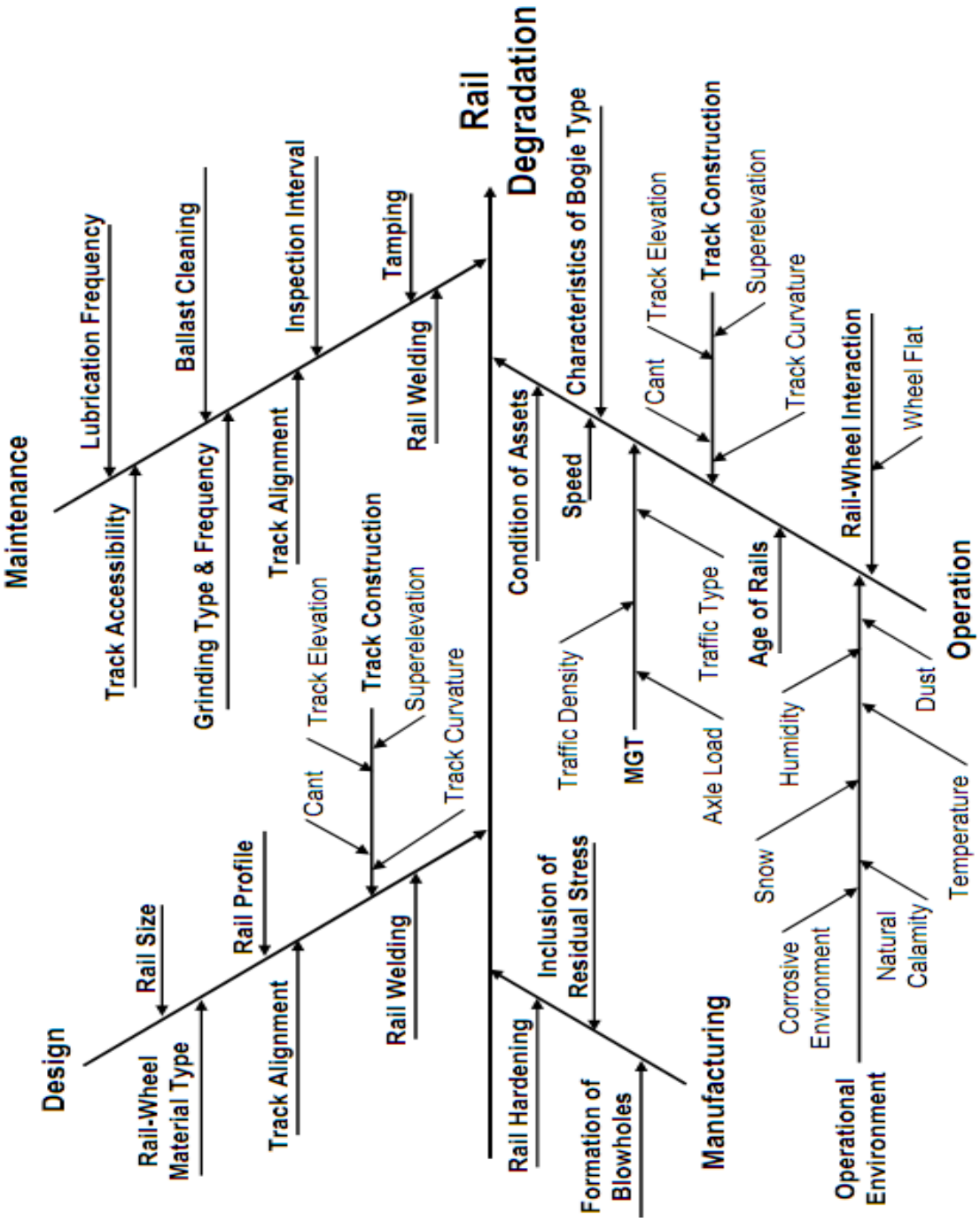

Figure 2.10 Cause and effect diagram for the factors influencing rail degradation (IHHA, 2001).

2.3.2. Types of Rail Damages

2.3.2.1. Rail Corrugations

Rail corrugations are cyclic (wave-like), generally vertical, irregularities on the running surface of the rails. Corrugations are of concern because they increase the dynamic wheel loads (and vibration), and therefore the rate of deterioration and failure of various track and vehicle components. The higher dynamic loads also increase the rate of corrugation development and the rate of rail profile deterioration. The rails therefore require more maintenance effort (grinding) at shorter intervals. Corrugations also increase, considerably, the wheel/rail noise. Corrugations are either short or long pitch (Australian Rail Track Co., (2006)).

Short pitch corrugations generally develop under lighter nominal axle load (< 20 tonnes) passenger operations with wavelength 30mm-90mm and the depth is usually less than 0.2-0.3mm. They are thought to form from the differential wear caused by a repetitious longitudinal sliding action of the wheel on the rail, whether through acceleration, braking or lateral motion across the rail.

Figure 2.11 short pitch corrugations on the running surface (U.S.DOT, 1984)

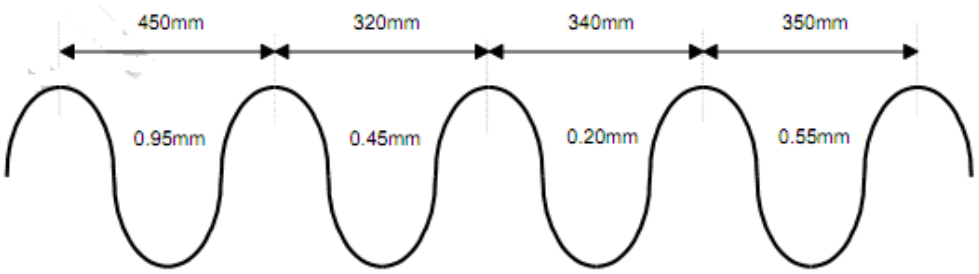

Figure 2.12 vertical profile of some long pitch corrugations (U.S.DOT, 1984)

Long pitch corrugations generally develop under higher nominal axle load (> 20 tonnes) mixed freight or unit train operations with wavelength of 300mm and the depth range from 0.1mm to above 2.0mm, and can be variable.

Figure 2.13 Rail plastic flow associated with long pitch corrugations (U.S.DOT, 1984)

2.3.2.2. Rolling Contact Fatigue Defects

Rolling contact fatigue (RCF) defects develop in rails on most Railway Systems and it describe a range of defects that are due, basically, to the development of excessive shear stresses at the wheel/rail contact interface. RCF defects that occur in the gauge corner region of the rails, and which are of most concern, may be Gauge corner checking or Shelling (Cannon, D.F., Edel, K.O., Grassie, S.L. and Sawley, K. (2003)).

Gauge corner checking is a surface condition that occurs mainly on the high rails in sharper curves, and can be described as being like “fish scales”. The cracks are initiated at or very close to the rail surface, typically occur at about 2-5 mm intervals along the rail, and can grow to 2-5 mm in depth.

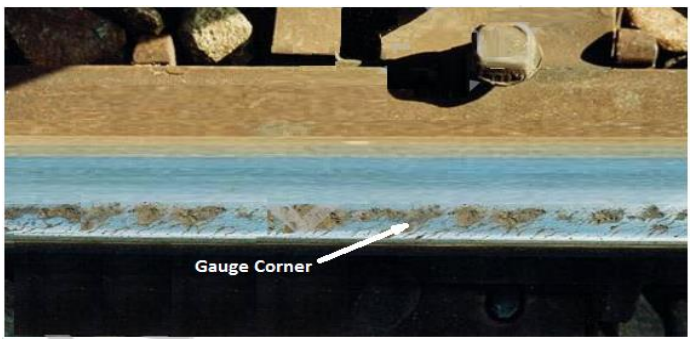

Figure 2.14 Severe stage of gauge corner checking cracks and spalls (U.S. Dept. of Transportation, 1984)

Shelling is an internal defect that initiates at a depth of 2-8mm below the gauge corner of, generally, the high rails in curved track. In the initial stages of development, shelling defects become noticeable as dark spots in the gauge corner region of the rails. Because of their internal nature, transverse defects cannot be visually detected, and hence must rely on regular ultrasonic rail inspection.

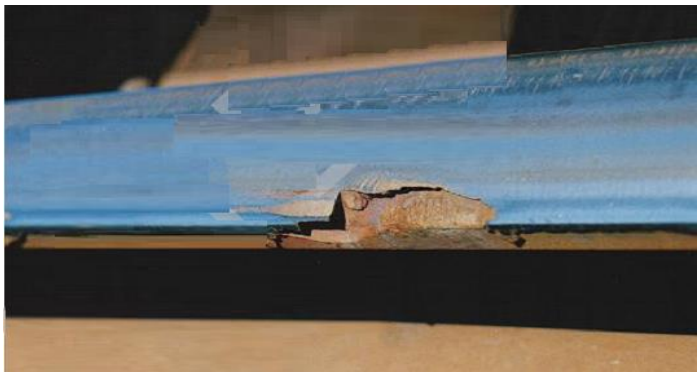

Figure 2.15 Severe stage of shell development (U.S. Dept. of Transportation, 1984)

2.3.2.3. Squat Defects

Squats are surface or near-surface initiated defects, which can be of two types. The more common type of squats, which are initiated on the crown or ball of the rail head and Squats that are initiated from the gauge corner checking cracks. Both types of squats develop mainly in shallower curves and tangent track, and in hardened rails (Cannon, D.F., Edel, K.O., Grassie, S.L. and Sawley, K. (2003)).

Figure 2.16 Rail Crown Squats (U.S. Dept. of Transportation, 1984)

2.3.2.4. Tache Ovale or Shatter Cracking

Tache ovales or shatter cracks (also known as transverse fissures) are internal defects that initiate near the center of the rail head at much greater depths, and grow transversely. As for transverse defects, because of their internal nature, tache ovales cannot be visually detected, and hence must rely on regular ultrasonic rail inspection. The initiation of tache ovale defects is due to the presence of excessive levels of hydrogen in rail steel (or welds) (Australian Rail Track Co., (2006)).

Figure 2.17 Tache Ovale Defect (Australian Rail Track Co., (2006))

2.3.2.5. Vertical Split Head

Vertical split head defects are vertical separations in the rail head, which tend to split the rail head in two parts and generally exist near the center line of rails, and can be of considerable length (>0.5-1.0m). Generally, small and medium defects cannot be detected visually (Australian Rail Track Co., (2006)).

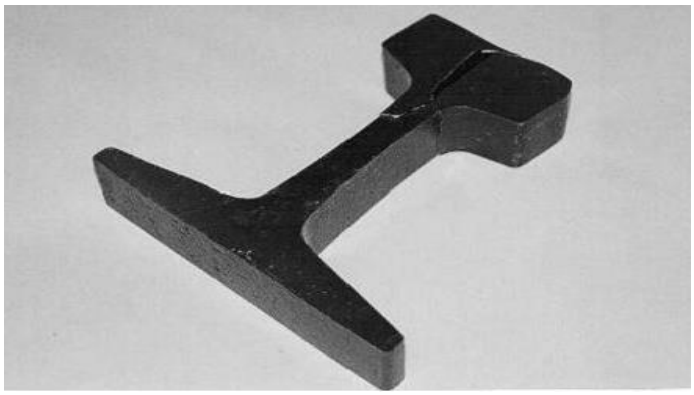

Figure 2.18 Vertical Split head defect (Australian Rail Track Co., (2006))

2.3.2.6. Horizontal Split Head

Horizontal split head defects are horizontal separations in the rail head, which tend to split the rail head in two parts. The defects initiate on the field side of the rails, at a considerable depth from the running surface (10-15 mm) and grow horizontally (parallel to the running surface), both across and along the rail head. It can be of considerable length (>50-100 mm). Generally, small and medium defects cannot be detected visually (Australian Rail Track Co., (2006)).

Figure 2.19 Horizontal Split Head defect (Australian Rail Track Co., (2006))

2.3.2.7. Wheel or Engine Burns

Wheel burns are defects that form on the running surface of the rails. Small wheel burns always occur in pairs directly opposite to each other on the two rails. Severe wheel burns, which can be more than 50 mm in length, exhibit what seem to be longitudinal gouging marks on their surface. Wheel burns can also occur while the locomotives are in motion. In this case, the damaged region can extend over a substantial length of the rail surface (Australian Rail Track Co., (2006)).

Figure 2.20 General appearance of Wheel Burns (Australian Rail Track Co., (2006))

2.3.3. Track Geometry Degradation at Transition Zone

2.3.3.1. Track settlement

When a track is loaded by the weight of the train and, superimposed to that, high-frequency load variations, the ballast and sub-ground may undergo non-elastic deformations. When unloaded, the track will not return exactly to its original position but to a position very close to the original one. After thousands and thousands of train passages, all these small non-elastic deformations will add, differently in different parts of the track, to give a new track position. This phenomenon is called differential track settlement. The track alignment and the track level will change with time. Depending on the sub-ground, the wavelength of these track irregularities will be of the order of meters up to hundreds of meters. The uneven track will induce low-frequency oscillations of the train. Succeedingly, the track load variations will increase and so will the track settlement. Especially, the transition area from an embankment to a bridge is a place where track settlements use to occur (Y. S. Kang, S.C. Yang, H.S. Lee, E. Kim, (2006)).

2.3.3.2. Deteriorations at Transition Zones

Bridge approaches and other track transitions such as road crossings and slab tracks to ballasted tracks are common locations of accelerated track geometry degradation differential settlement. Accelerated track geometry degradation in these localized areas can lead to increased costs to railroads due to maintenance, train delays, or speed restrictions. Other negative impacts include increased wear and tear on the bridge, track, and vehicle components, as well as decreased ride quality for sensitive freight and passengers (Iwnicki S. 2006).

Three major causes or factors for the above problems can be:

1. A large change in track stiffness from change in track structure leads to uneven track deflections under moving traffic loading that can have an adverse effect on dynamic vehicle/ track interaction. Increased forces in the track cause or accelerate uneven settlement, which leads to even higher forces, depending on

A. the elevation change, which is related to the change of the stiffness
B. the train speed
C. the vehicle mass
D. the suspension characteristics of the vehicle

2. The ballasted approach section inherently settles more than the bridge section because of underlying soil layers, thus producing an uneven profile or differential settlement that leads to adverse dynamic vehicle/track interaction. Li and Selig (1995) report on plastic deformation of ballast and substructure layers. Excessive and rapid accumulation of plastic deformation leads to an excessive rail settlement, and thus requires frequent maintenance.

3. Geotechnical issues, such as poor materials, inadequate compaction and consolidation of the fill and embankment, and poor drainage conditions.

Due to the relationship between the dynamic load of the running trains and the track deflection, the track geometry in the transition zone can deteriorate at an accelerating rate through a self-perpetuating mechanism; as the dynamic load increases so does the track differential settlement, which in turn leads to even higher dynamic forces and soon.

For comparison purposes, let us divided a bridge site into three sections as the track on bridge, the approach track (within 30 m or 100 ft. from the bridge abutments) and open track (beyond 30 m or 100 ft. from the bridge abutments).

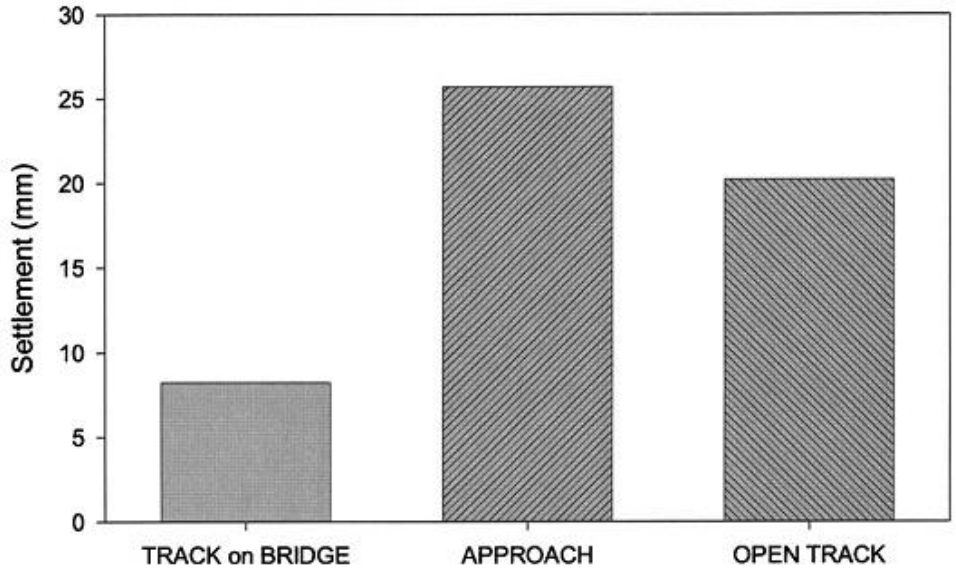

Figure 2.21 Comparison of track settlements over one maintenance interval (Selig and Li, 1994)

2.3.4. Crack Growth Model

P. Paris and F. Erdogan 1963, many fatigue life analysis have applied the Miner's damage accumulation law or some specific PDFs (Probabilistic Density Functions) such as the Weibull and Exponential distributions, to predict the probabilistic life of a metallic material, since the models accordingly represent the characteristics of the material. However, railroad companies usually use a crack size as the inspection results. Therefore, it is hard to deal with reflecting the results of the inspections and repair strategy in their approach because they do not provide information about crack size. A qualitative analysis for the rail reliability needs the knowledge of the crack size at arbitrary times, so a crack growth model based on linear elastic fracture mechanics is employed here instead of the Miner's damage accumulation and a specified PDF model in this thesis.

The crack growth model used in this study is based on Paris and Erdogan's law, where the rate of crack growth is defined as

$$\frac{da}{dN} = C(\Delta K)^m \quad \text{----------2.14}$$

Where, a is the crack size, N is the number of stress cycles, C and m are material parameters, and ΔK is the stress intensity factor range. According to linear elastic fracture mechanics under a constant amplitude loading, ΔK can be computed as

$$\Delta K = K_{max} - K_{min} = YS\sqrt{\pi a} \quad \text{----------2.15}$$

Where, Y is the geometric correction factor and S is the tensile stress range, also called the far-field stress range.

It is noted that the use of the stress intensity factors implies that equation (2.15) only applies to essentially elastic situation, so that the factor provides a reasonable description of the crack tip stress field for a distance up to 0.1a from the crack tip.

2.3.5. Countermeasures for track stiffness irregularities

In order to construct a transition zone with the desired variation of stiffness and geometry there are some possibilities (T. Dahlberg, 2010);

- Use of Geosynthetic reinforcements
- Use supplementary (Auxiliary) rails
- Use of elastomeric products, such as rail pads, under sleeper pads (USP), and sub-ballast mats (SBM),
- Use of approach slabs
- Chemical treatment of sub-soil
- Management of the ground water
- Use of fastenings with varying elasticity

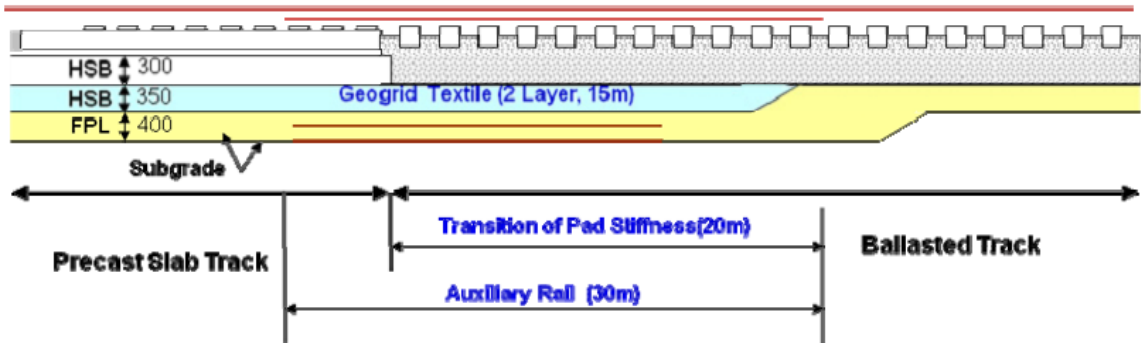

Figure 2.22 Performance improvements of transition track on Site (Y.S.Kang, S.C. Yang, H.S. Lee, E. Kim, (2006))

Some of the track stiffness irregularities smoothening techniques are:

- Use of Geosynthetic reinforcements like geotextiles, geogrids, geonets, geomembranes, geosynthetic clay liners, geofoam, geocells and geocomposites.
- Use of supplementary (Auxiliary) rails enable for train vehicles to operate smoothly between slab track and ballasted track. Auxiliary rails were combined on the precast slab for 5.2 m section and the 30 m rails will be extended to the ballasted track.
- Use of elastomeric products, such as rail pads, under sleeper pads (USP), and sub-ballast mats (SBM), can also help for the uniform and gradual change in track modulus. The elastic change of pad stiffness may be applied to lessen the subsidence of the track by changing the elasticity for instance from 22.5kN/mm to 50kN/mm in 5 steps. The substructure of slab track as HBL (Hydraulically Bonded Layer) and FPL (Frost Protection Layer) may also be elongated for prevention of subsoil settlement (Selig and Li 1994; Redden et al. 2003).

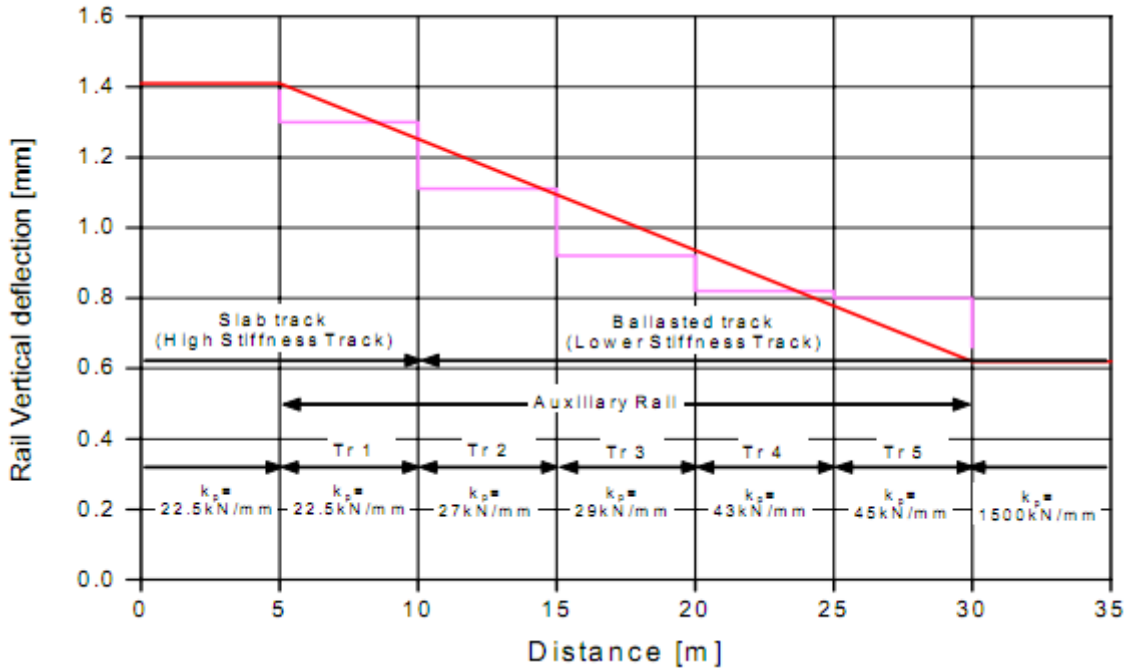

Figure 2.23 varying rail pads stiffness provision in transition zone (Y.S.Kang, S.C. Yang, H.S. Lee, E. Kim, (2006))

2.4. Track Maintenance

Railway lines are investments with very long life. Today many tracks are over 100 years old. Of course components have been exchanged during the years, but parts of the track might remain the same – especially the substructure. Typical lifetimes of for example rails are 30 – 60 years and turnouts 20 – 30 years (H. Sundquist, 2000). However, to ensure this long life a large amount of maintenance is necessary.

There are several, quite obvious reasons for maintenance, for example:

- Safety – Probability for accidents needs to be low.
- Comfort – Comfort is important, both for passengers and freight as well as for the environment in terms of noise and vibration.
- Availability – With lots of failures and speed restrictions due to safety etc. the availability of the track will be low.
- Economy – A track with low quality is cost driving, since the deterioration of both track and trains will be higher. At the same time maintenance is expensive. Optimization and Life Cycle Cost (LCC) planning is needed.

Regarding remedial actions accompanied with rail inspections, the Japanese rail road company JR East establishes the rules shown in tables below which explains the rules

ratified by Department of Transportation (DOT) for reference. JR East institutes the rail inspection rules for each unit rail, basically 25m.

Table 2.2 Remedial Action Table in JR East

Types of Defects	Criteria [mm]	Remedial action
Vertical split head	$5 \leq a < 15$	Marking for check
	$15 \leq a < 30$	Apply bolted joint bar and plan to replace
	$30 \leq a$	Replace immediately
Split web	$2 \leq a < 6$	Marking for check
	$6 \leq a < 10$	Apply bolted joint bar and plan to replace
	$10 \leq a$	Replace immediately
Broken Base	$a < 3$	Apply bolted joint bar and plan to replace
	$3 \leq a$	Replace immediately
Bolt-hole crack	$a < 5$	Marking for check
	$5 \leq a$	Replace immediately

Table 2.3 Remedial action Table in DOT

Types of Defects	Criteria [mm]	Remedial action
Vertical split head	$2.54 \leq a < 5.08$	Limit operating speed over defective rail to 48 [km/h]
		Inspect the rail 30 days after it is determined to continue the track in use
Split web	$10.16 \leq a$	Limit operating speed as authorized by track supervisor
		Operating speed cannot be over 48 [km/h]
Broken Base	$2.54 \leq a < 15.24$	Apply joint bars bolted within 10 days after it is determined to continue the track in use
		After applying the jointed bars, limit operating speed to 80 [km/h]
Bolt-hole crack	$2.54 \leq a < 3.81$	Limit operating speed over defective rail to 80 [km/h]
		Inspect the rail 30 days after it is determined to continue the track in use

JR East set up rules by which the track engineers have to replace the rail at 400 Million Gross Tones (MGT) with new one.

3. Finite Element Modeling and Analysis

3.1. Introduction

This chapter deals with modeling of a 2D geometry of the whole track (showing both the embankment/ballasted and slab/ballastless sections at the transition zone) and a 3D rail in ABAQUS software. The 2D model is for stress and settlement analysis (to examine the stress increment at transition sections) and the 3D rail model is for crack analysis in FRANCE 3D software. So in order to accomplish the above task, choice of an appropriate geometry of track components, selection of material and property assignments, loading of the track and its analysis are required. A brief summary of the routines that have been used in the analysis are presented.

3.2. Modeling in ABAQUS/CAE

The ABAQUS Software is a product of Dassault Systems Simulia Corp., Providence, RI, USA. ABAQUS/CAE (Complete ABAQUS Environment) is used to create complex models, analyze and visualize results following the procedures shown in the figure 3.1. It contains nine modules which needs to be followed in order to get expected output. These modules are: Part, Property, Assembly, Step, Interaction, Load, Mesh, Job, and Visualization.

3.2.1. Two-Dimensional Transition Zone ABAQUS Model

The 2D transition section ABAQUS model analyzed in this research paper considers only half geometry (the embankment modeled on the left side and the slab bridge modeled on the right side) of the actual transition zone. The reason behind taking only half section are, first the model is x-symmetric so that if we analyze half of the section then the results will be more or less repeated on the right side (Ivo Seara, 2007) and second if I consider the whole zone (a slab between two embankments) the time needed for analysis will be very long so I take only half model.

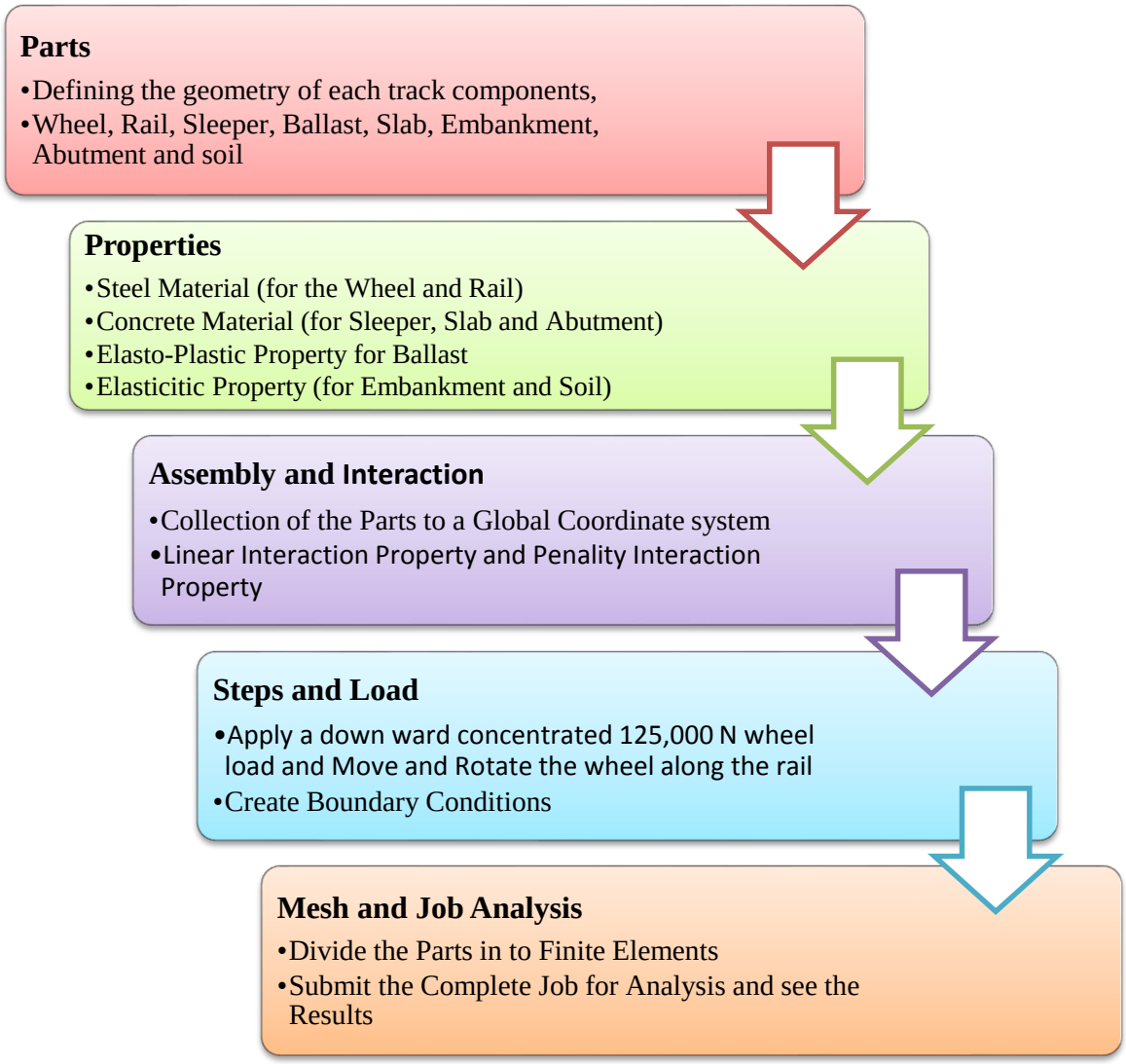

Figure 3.1 ABAQUS Modules for Modeling and Analysis

3.2.1.1. Geometry and Material Properties of Track Components

✓ **Wheel**

The wheel is modeled as a wire element and the wheel center (which is assigned as a reference point) acts as a center of rotation.

Table 3.1 wheel modeling parameter values

Symbol	**Name**	**Unit**	**25 t Axle Model**
Mw	Mass of Wheels	Kg	300
Iwx	The wheel moment of inertia about the X-axis	$Kg.m^2$	700
Iwy	the wheel moment of inertia around the Y axis	$Kg.m^2$	100
Iwz	The wheel moment of inertia around the Z axis	$Kg.m^2$	700
ρ	Density	kg/m^3	7850
E	Modulus of elasticity	Gpa	210
γ	Poisson's ratios		0.3
D	Diameter	Mm	840

✓ **Rail**

The rail was modeled as a beam element with simplified cross-sectional dimensions and 42.5m length. Its density is taken as 7850 kg/m^3, modulus of elasticity is 210GPa, and Poisson's ratios is 0.3. For the determination of stress in rail material due to the moving train, rail is modeled by Winkler's beam on elastic foundation theory, as a beam supported by a continuous distribution of springs along the length of the beam, as shown in Figure

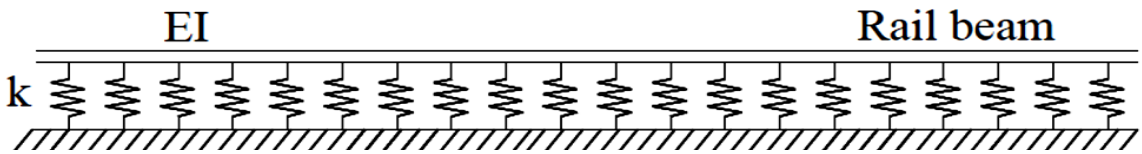

Figure 3.2 Schematic representation of beam on elastic foundation model (Esveld, 2001)

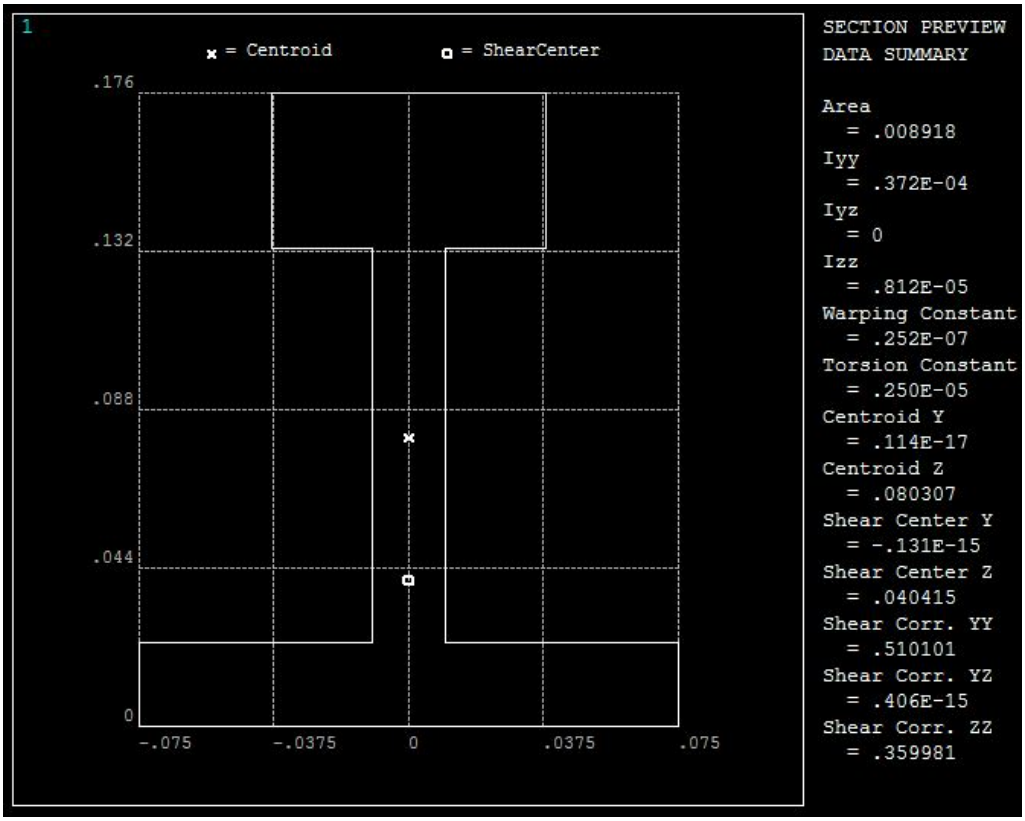

Figure 3.3 simplified cross-section of 60 kg/m rail

✓ **Rail Pad**

In this thesis the following values were taken from literatures

Table 3.2 Rail Pad modeling parameter values

Component	**Parameters**	**Values**
Rail Pad	Stiffness (K)	200*e6N/m
	Damping (C)	50*e3Ns/m
	Height	0.075m

✓ **Sleepers**

Some of the basic parameters of sleeper are shown in Table below for the general line, sleepers configuration 1760 / km or 1,840 / km, corresponding sleeper spacing LS = 0.568m or LS = 0.545m. In this thesis, 200km per hour or more for new high-speed railway, sleepers configured for **1667 / km, the sleeper spacing LS = 0.6m.**

Table 3.3 The basic parameters used for sleepers

Main types	Sleeper quality, ms/kg	Sleeper length, ls/m	The average width of the bottom, lb/m	Effective supporting length (half-pillow), le/m
ordinary wooden sleepers	100	2.5	0.19-0.22	1.1
Existing concrete sleepers (I type)	237	2.5	0.267	0.95
Wide concrete sleepers (76 chord type）	520	2.5	0.55	0.95
Speed trunk sleeper (II type）	**251**	**2.5**	**0.27**	**0.95**
Passenger sleeper (III type）	340	2.6	0.29	1.175

In addition to the above parameters, density = 2500kg/m^3, modulus of elasticity = 34 GPa, Poisson's ratios is 0.2 is considered.

- ✓ **Ballast**

The ballast is modeled as an elasto-plastic material having the Drucker–Prager yield criterion (DP). DP is a pressure-dependent model for determining whether a material has failed or undergone plastic yielding. The yielding surface of the DP criterion may be considered depending on the internal friction angle of the material and its cohesion. But in this project work the ballast material is considered to be cohesion less since it is a granular material.

Flow Stress Ratio (k) is the ratio of the yield stress in triaxial tension to the yield stress in triaxial compression. The value of k in the linear Drucker-Prager model in ABAQUS is restricted to $1 \geq k \geq 0.778$ and a value of k= 0.8 is used in this project model.

In this thesis the parameters considered to model the 2D ballast section are:

Table 3.4 Parameters used to model ballast

Material	Ballast
Density (Kg/m^3)	1500
Elastic Modulus, E(Mpa)	100
Poison's ratio, γ	0.3
Dilation angle, ψ	33^0
Angle of internal friction, φ	55^0
Flow stress ratio, k	0.8
Depth (m)	0.35
Length (m)	30

✓ **Bridge Slab**

The bridge slab is modeled as a 2D model having 0.7m depth and 12.5m length (dimensions are taken from Chinese Standard), other slab parameters include like: Density is taken as 2500Kg/m^3, Elastic Modulus (E) is 34*e9 Pa and Poison's ratio (γ) is 0.2.

✓ **Embankment**

The embankment is also modeled as 2D having 5m depth and 30m length (dimensions are taken considering effective transition length (10-20m away from bridge slab) and from different literatures), other parameters include: Density is taken as 1700Kg/m^3, Elastic Modulus (E) is 1*e8 Pa and Poison's ratio (γ) is 0.3.

✓ **Abutment**

2D model of the abutment has 2m length and since the top riding surface need to be smooth

- Height of Abutment = (Hembankment + Hballast) – Hslab
  = 5m + 0.35m – 0.7m
  = 4.65m

The other abutment parameters used in modeling are Density is 2500Kg/m^3, Elastic Modulus (E) is 20*e9 Pa and Poison's ratio (γ) is 0.2.

✓ **Soil**

The last bottom supporting track component is the soil which is also modeled as 2D with Density = 1700Kg/m^3, Elastic Modulus (E) = 1*e8 Pa and Poison's ratio (γ) = 0.3

3.2.1.2. Assembly and Interaction of track components

➢ **Assembly**

When we create a track component (part), it exists in its own coordinate system, independent of other track component (parts) in the model. In contrast, in this assembly section we create instances of our track components and position the instances relative to each other in a global coordinate system, thus creating the assembly. We position track component instances by sequentially applying position constraints that align selected faces, edges, or vertices or by applying simple translations and rotations.

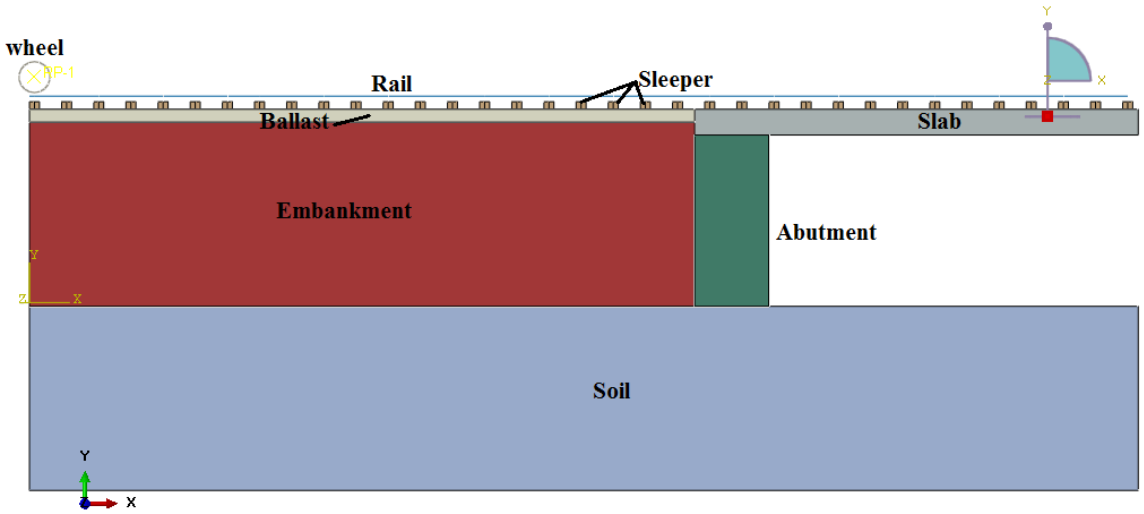

Figure 3.4 Half 2D Transition Zone Assembly Model

➢ **Interaction of Track Components**

In order to move and rotate the wheel a rigid body constraint is applied for the wheel at the reference point which needs to be created at the center of the wheel. Since we are doing 2D analysis all the three degree of freedoms i.e. in x, y, and z-axis must be constrained to move together.

In addition to the above interaction, in this thesis two contact properties were used. One is between the wheel and the rail which has linear pressure-over closure normal behavior and penalty friction formulation tangential behavior (with 0.8 friction coefficient). The

second contact property is between the other track components (other than wheel and rail) with "Hard" contact pressure-over closure normal behavior and penalty friction formulation tangential behavior (with 0.8 friction coefficient).

3.2.1.3. Loading and Boundary Conditions

The explicit dynamics procedure type has been used for step calculation in this thesis. The explicit scheme appeared to be very computationally demanding and is more appropriate to use when the time interval is very small. However it is easier to achieve convergence based on an explicit scheme if the behavior of the structure is unknown.

- The loadings in the 2D track model were applied in two steps:
  - ❖ The first step is to apply a concentrated 125,000 N down ward wheel load on the reference point of moving rigid wheel with a time period of 0.1 second.
  - ❖ The second is to move and rotate the wheel along the rail. But in this case I ignore the rotation because it doesn't make significant difference rail stress determination due to steady-state analysis. The time can be found as follows:

$$speed = \frac{distance}{time}, \Longrightarrow time = \frac{distance}{speed}$$

But, Total length covered by wheel = length of the rail = 42.5m

Design speed = 200 km/hr = 55.5 m/s

Therefore, $time\ period = \frac{distance}{speed} = \frac{42.5m}{55.5\ m/s} = 0.76\ second$

Boundary conditions considered in this research are:

- All the 2D track model components are only allowed to move (displace) vertically i.e. in y-axis, so the model is restrained on left and right side because of continuity.
- Encastre restraint is applied at soil bottom part (not to move in all x, y, and z direction i.e. U1 = U2 = U3 = UR1 = UR2 = UR3 = 0).

3.2.1.4. Meshing

The two dimensional transition section model considered in this thesis consists of 15455 number of nodes and 8553 number of elements. The mesh size consideration is limited with analysis time and result accuracy. Consequently, we couldn't take finer mesh size for all parts because it needs more analysis time and also on the contrary I couldn't take

courser mesh size as the results will be rough so it needs optimization. Since I need more accurate result on top part of the track structure, especially on the rail, the mesh size considered for the wheel, the rail and sleepers were relatively finer as compared with the ballast, bridge slab, embankment, abutment and soil. The mesh sizes taken for the wheel, rail and sleeper parts are 0.01m, 0.01m and 0.012m respectively and for that of ballast, bridge slab, embankment, abutment and soil parts it is 0.1m, 0.1m, 0.5m, 0.3m and 1m respectively.

3.2.2. Three Dimensional Rail Modeling for Crack Analysis

For the detail analysis of the effect of adverse stress increment at transition zone, caused by the abrupt support stiffness difference, a three dimensional rail model was done on ABAQUS software which then can be imported in FRANC 3D software for the crack analysis. For the analysis implementation, a rail of T-60 profile subjected to an amplified stress (at transition section) with 0.6m length was taken. The cause for choosing such a length was that the two sleepers could be placed underneath the rail at the standard distances of 0.6m.

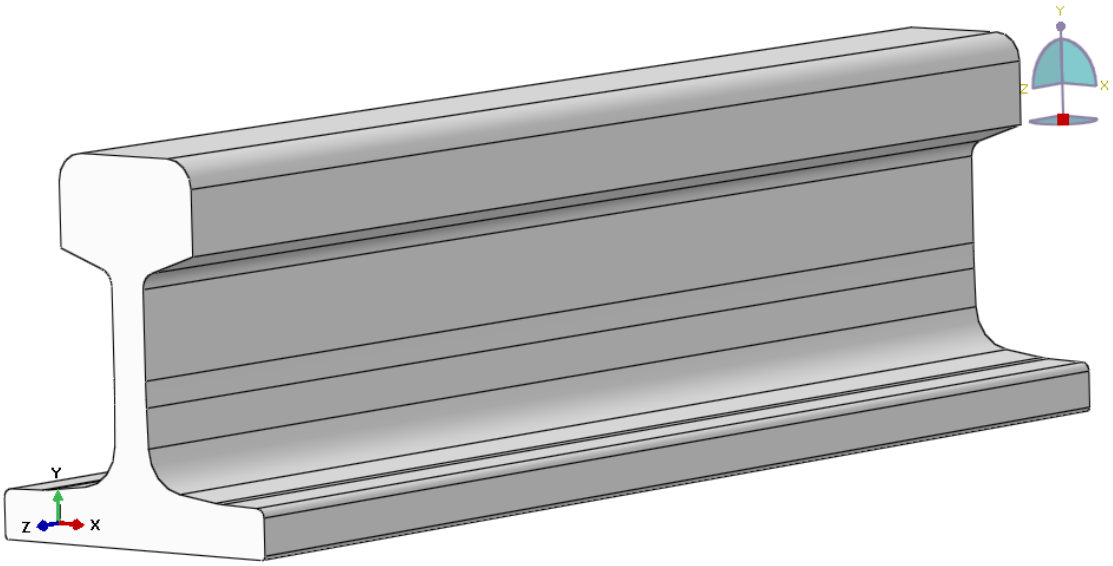

Figure 3.5 Geometric model of T-60 rail created by ABAQUS

Some of the parameters considered in the stress analysis include axle Load of 25t (250kN) and design speed of 200km/h as for mixed use train speed range is 160<v<200 km/hr.

Design Wheel Load

$P^D = \emptyset\ Ps$ …….3.1

Where P^D = design wheel load (KN),

Ps = static wheel load (KN), and

$\emptyset$ = dimensionless impact

$\emptyset$ (dimensionless impact factor) is always >l. The nominal vehicle axle load is usually measured for the static condition, but in the design of railway track the actual stresses in the various components of the track structure and in the rolling stock must be determined from the dynamic vertical and lateral forces imposed by the design vehicle moving at designed speed [Doyle, 1980]. Dynamic impact factor is a corrective factor to compensate for dynamic as well as impact effects of wheel load resulted from wheel and rail surface irregularities [Sadeghi and Barati, 2010].

Table 3.5 Recommended relationship for dynamic coefficient factors

Recommender	**Formula**
AREMA	$\emptyset = 1 + 5.21\frac{V}{D}$
DB	$\emptyset = 1 + \frac{V^2}{3 * 10^4}\ , for\ V\ \leq \frac{100km}{hr}$ $\emptyset = 1 + \frac{4.5 * V^2}{10^5} - \frac{1.5 * V^3}{10^7}, for\ V > 100km/hr$
India	$\emptyset = 1 + \frac{V}{58.14k^{0.5}}$
South Africa	$\emptyset = 1 + 4.92\frac{V}{D}\ , for\ narrow\ gage$

Where, V= Design Speed (km/hr), D=Wheel Diameter (mm), K = Track Modulus (MPa)

The axle load was chosen as 250KN.The load for each wheel will be:

$$Ps = \frac{Axle\ load}{2} = 125\text{KN}.$$

To determine the vertical wheel load on the rail, the dynamic impact factor expression recommended by AREMA was used and the vehicle speed was taken as 200 Km/hr and the wheel diameter as 0.84m (840mm).

$$\emptyset = 1 + 5.21\frac{V}{D} \text{ ……..3.2}$$

V (Design Speed) = 200 km/hr

D (Wheel Diameter) = 840mm

Hence, $\emptyset = 2.24$

Therefore, Design Wheel Load (P^D) $= \emptyset$ * *Ps* = 2.24*125kN = 280kN

Table 3.6 Rail material selection

S.N	Radii of Curvature(mm)	Gauge (mm)	Axle load (N)	Chinese Standard (Kg)	Poison's Ratio	Young's Modulus (GPa)
1	$R_1{}^W = \infty$	1435	250,000	60	0.3	210
2	$R_2{}^W = 300$					

$R_1{}^W$ and $R_2{}^W$ are explained in section 2.2.2.1

According to Hertzian contact theory, the contact surface between two curved surfaces, such as a wheel and a rail, can be represented as an ellipse with a major semi-axis a and minor semi-axis b. The pressure exerted over this elliptical area is parabolic in two directions and is defined according to the following equation:

$$Po = \frac{3}{2}\left(\frac{W}{\pi ab}\right) \text{----------3.3}$$

Where P_0 is the maximum contact pressure at the initial central contact point, W is the static wheel load, *Ps* (KN).

Depending on the size and orientation of the contact ellipse the positions of the contact point may be shifted in different directions based on the magnitude of x or y. However, based on the above general Hertz contact formula, the stress due to wheel/rail contact decreases and becomes zero if it goes far away from the centerline of the rail head. Similarly, the wheel/rail contact stress is inversely proportional to the major and minor axis of the contact ellipse.

The magnitudes of a and b also depend on the applied normal force, as well as the profile and materials of the wheel and rail. They are expressed as:

$$a = m\left[\frac{3\pi W(K_1+K_2)}{4K_3}\right]^{\frac{1}{3}}$$ ----------3.4

$$b = n\left[\frac{3\pi W(K_1+K_2)}{4K_3}\right]^{\frac{1}{3}}$$----------3.5

Where, W in this case is Design Wheel Load (P^D) = 280kN

$$K_1 = \frac{1-V_W^2}{\pi E_W}, \quad K_2 = \frac{1-V_R^2}{\pi E_R}, \quad K_3 = \frac{1}{2}\left(\frac{1}{R_1}+\frac{1}{R_1'}+\frac{1}{R_2}+\frac{1}{R_2'}\right)$$

Here Ew, Er, υ_w, and υ_r are the modulus of elasticity and Poisson's ratios of wheel and rail, respectively. R1 and R2 are defined as the principal rolling radii of the wheel and rail, respectively. R1' and R2' are the transverse radii of curvature of the wheel and rail, respectively.

In the above table,

- Poison's Ratio of wheel and rail (υ_w and υ_r) are given as 0.3 (both are steels)
- Young's Modulus (Ew, Er) = 210 GPa
- R1 = 420mm (840mm/2) and R2 = ∞
- R1' = ∞ and R2' = 300mm

Now computing for the above parameters we have:

K1 = 1.38 * 10^{-12} m^2/N

K2 = 1.38 * 10^{-12} m^2/N

K3 = 2.86 * 10^{-3}/mm

The coefficients m and n in the above equations are functions of θ.

The variable θ is defined as:. $\theta = \cos^{-1}\frac{K_4}{K_3}$ ----------3.6

Where,

$$K_4 = \frac{1}{2}\left[\left(\frac{1}{R_1}+\frac{1}{R_1'}\right)^2+\left(\frac{1}{R_2}+\frac{1}{R_2'}\right)^2+2\left(\frac{1}{R_1}-\frac{1}{R_1'}\right)\left(\frac{1}{R_1}-\frac{1}{R_1'}\right)\cos 2\varphi\right]$$----------3.7

and φ is the angle between the normal planes that contain the curvatures 1/R1 and 1/R2 also called yaw rotation. For this thesis φ is taken as 0 (because for a straight segment the curvature of the rail is zero degree).

Inserting the above values for R1, R2, R1' and R2',we can get:

K4 = 4.76 * 10^{-4}/mm

Then, θ will be:

$$\theta = \cos^{-1}\frac{K_4}{K_3} = \cos^{-1}\left(\frac{4.76e{-}4}{0.00286}\right) = 80.4$$

By using linear interpolation method for hertz coefficients (shown in table A-2), the value of m and n for the chosen rail can be easily obtained as follows:

$\theta_1 = 80^0$, m_1=1.128, n_1=0.893; $\theta_2 = 85^0$, m_2=1.061.n_2=0.944

Therefore, for $\theta = 80.4^0$, m = 1.123 and n = 0.897

Now a and b can be obtained to be, a = 0.01m and b = 0.0081m

By using the values of a and b, the hertz stress contact pressure will be:

Po = 1650.5 MPa

To determine the size of the contact area, determination of the orientation of the shape of the contact ellipse is necessary.

$$\frac{1}{R_1^W} + \frac{1}{R_1^r} \geq \frac{1}{R_2^W} + \frac{1}{R_2^r} \gg \frac{1}{420} + \frac{1}{\infty} \leq \frac{1}{\infty} + \frac{1}{300}$$

Therefore, the transverse semi axis of the contact ellipse (y direction) is less than or equal to the longitudinal semi-axis. The contact ellipse major axis a is along the length of the rail and the contact ellipse minor axis b is along the width of the rail.

The result contact area was an ellipse with a contact patch area of **π*a*b=2.545*$10^{-4}$$m^2$**. From equation 2.3, the equation for the resulting pressure distribution is

$$P = 1650.5 * e6N/m2\sqrt{1 - \left(\frac{x}{0.01}\right)^2 - \left(\frac{y}{0.0081}\right)^2}$$

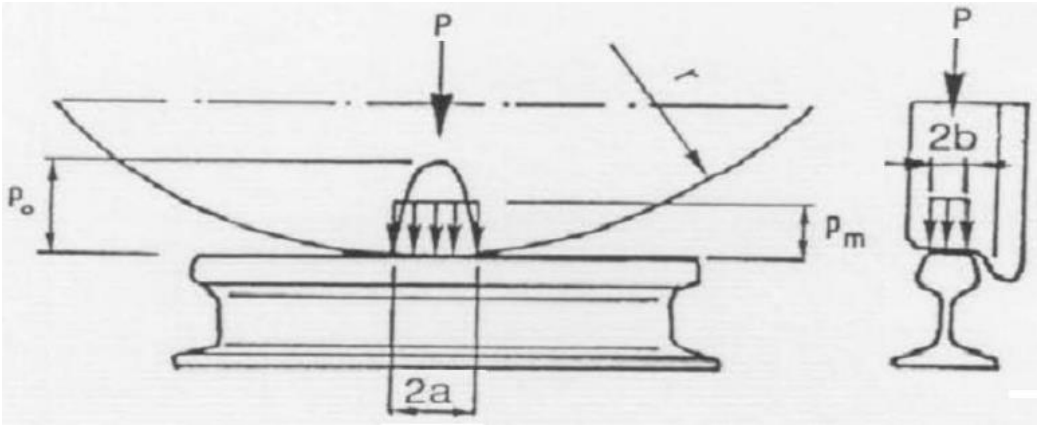

Figure 3.6 wheel rail contact pressure distribution (Esveld, 2001)

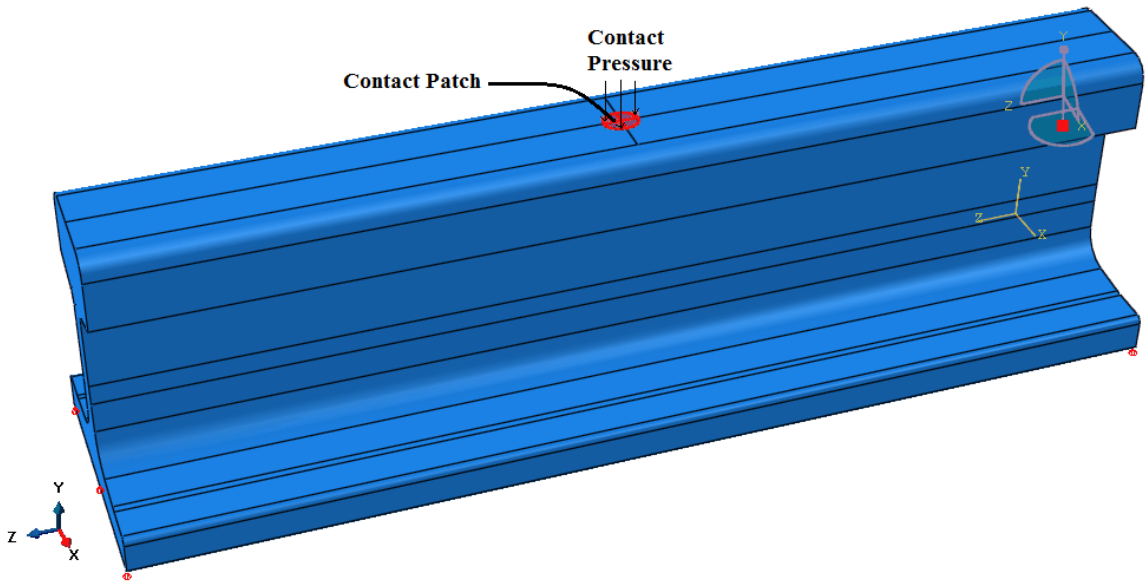

Figure 3.7 Contact Pressure applied on elliptical contact patch

However, the pressure we get from the above analysis i.e. the hertz stress contact pressure (Po = 1650.5MPa) is on a normal track section where there is no sudden variation in track modulus but the intention of this research is to study the influence of the stress increment when the train pass from bridge (higher track modulus) to embankment (lesser track modulus) at transition section which is due to abrupt support stiffness difference. Therefore, this stress increment needs to be determined from the results of the above 2D transition section Abaqus model that is found in the next "Results and Discussions" chapter.

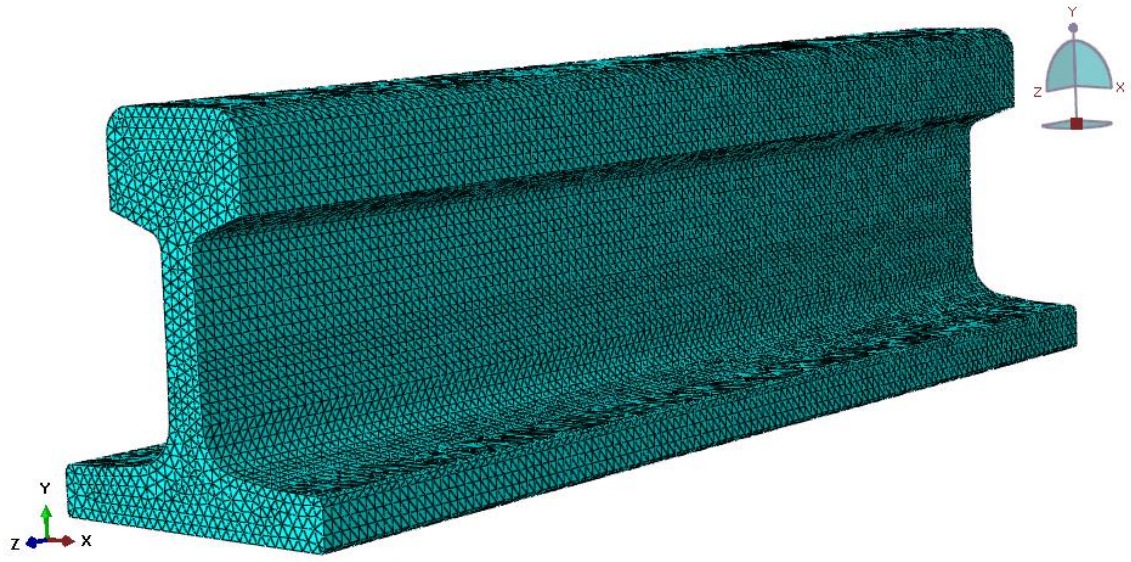

Figure 3.8 Finite Element mesh of the rail model in ABAQUS

The three dimensional rail model considered here consists of 70699 number of nodes and 45178 number of elements. Even if analysis time required is long the mesh size considered is fairly finer because we need accurate results.

4. Results and Discussions

4.1. Introduction

In the previous chapters, the theoretical background (literature review) to deal with the research problem, and a technique of developing a model for analysis are outlined, here in this chapter analysis results and a discussion of the analysis results is presented. First, the general track performance at transition section where a large abrupt stiffness variation exhibited under moving loading is discussed with the corresponding stress and settlement effects. In this section the stress intensity difference between the embankment section and bridge section will be analyzed and compared with stress intensity visualized on normal track sections where there is no abrupt stiffness variation found on previous research works. Then holding this stress variation which amplifies the dynamic effect of the moving wheel on the rail we will try to determine the expected crack on rails at the transition location using fracture analysis software FRANCE 3D.

4.2. Track Performance at Transition Section

4.2.1. Stress on the Rail at Transition Section

From previous studies, the maximum stress on normal track section where there is no abrupt stiffness variation ranges between 115MPa – 120MPa. But in the present research work, from the ABAQUS software output, the stress on the rail is found to be 126.7MPa as shown in the figure 4.1 below.

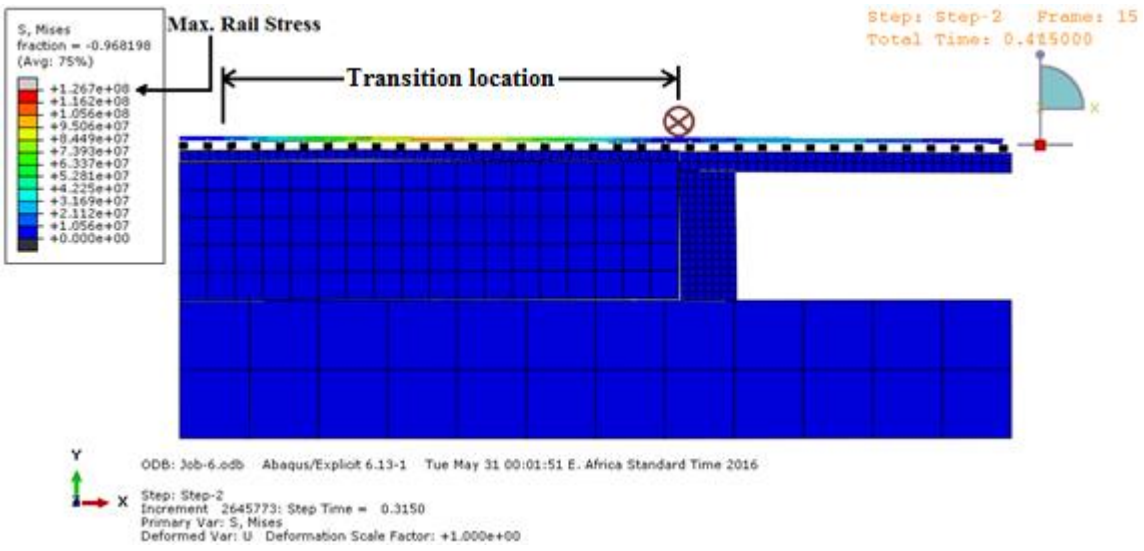

Figure 4.1 ABAQUS Rail Stress result (for forward speed of 200km/hr)

Figure 4.2 stress (MPa) variation along the length (m) of the track (when the wheel moves from bridge to embankment) for speed of 200km/hr

As we see from the above figure 4.1 and 4.2 there is higher stress concentration on the embankment location than the bridge location due to smaller support stiffness on the embankment section. Consequently, the deflection (settlement) response follows the stress distribution. As we can see from figure 4.5 and 4.6, on the left side embankment section (on ballasted track) deflection is higher than right side bridge section (ballstless or slab track). So due to this higher stress concentration on embankment side the rail is exposed to high bending stress.

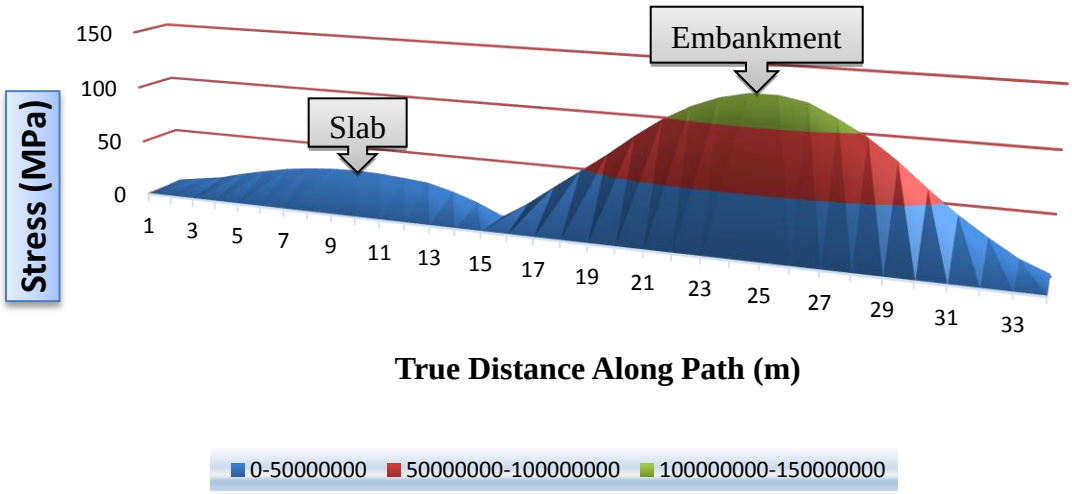

Figure 4.3 stress (MPa) variation along the length (m) of the track for backward speed of 200km/hr

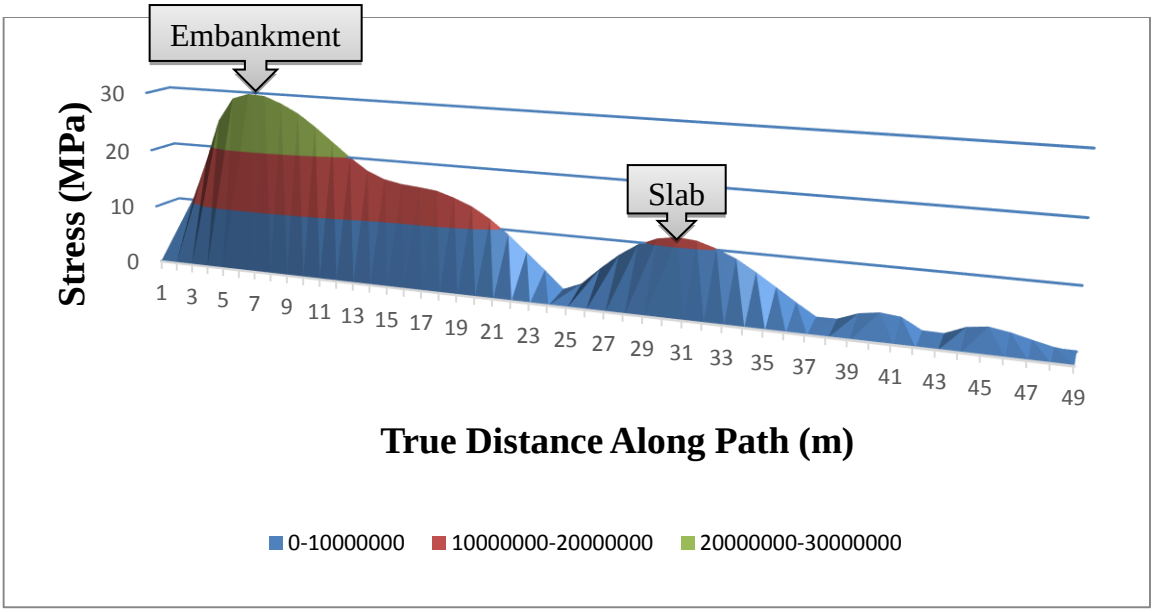

Figure 4.4 stress (MPa) variation along the length (m) of the track for forward speed of 160km/hr

Therefore, we can see that, the maximum stress variation occurs for speed of 200km/hr than that of 160km/hr. However, the stress in the rail should not exceed the allowable.

Allowable Bending Stress in the Rail

The Association of American Railroads recommends that acceptable rail stress for continuous welded rail be established as:

$$\sigma_{all} = \frac{\sigma_y - \sigma_t}{(1+A)(1+B)(1+C)(1+D)}$$ ----------4.1

Table 4.1 Acceptable Rail Stress for Continuous Welded Rail (adopted from AREMA)

Reduction Factor	Severity Assumption
A. Lateral Bending	20%
B. Track Condition	25%
C. Rail Wear Corrosion	15%
D. Unbalanced Elevation	15%
σ_t. Temperature Stress	20,000 psi (138MPa)

σy = 74 ksi (510MPa)----------AREMA table 4-2-1-4-1c

$$\sigma_{all} = \frac{510MPa - 138MPa}{(1+0.2)(1+0.25)(1+0.15)(1+0.15)} = 187.52MPa$$

So the stress we get at transition section (126.7MPa) is less than $\sigma_{all}(187.52MPa)$ (ok!)

4.2.2. Rail Settlement at Transition Section

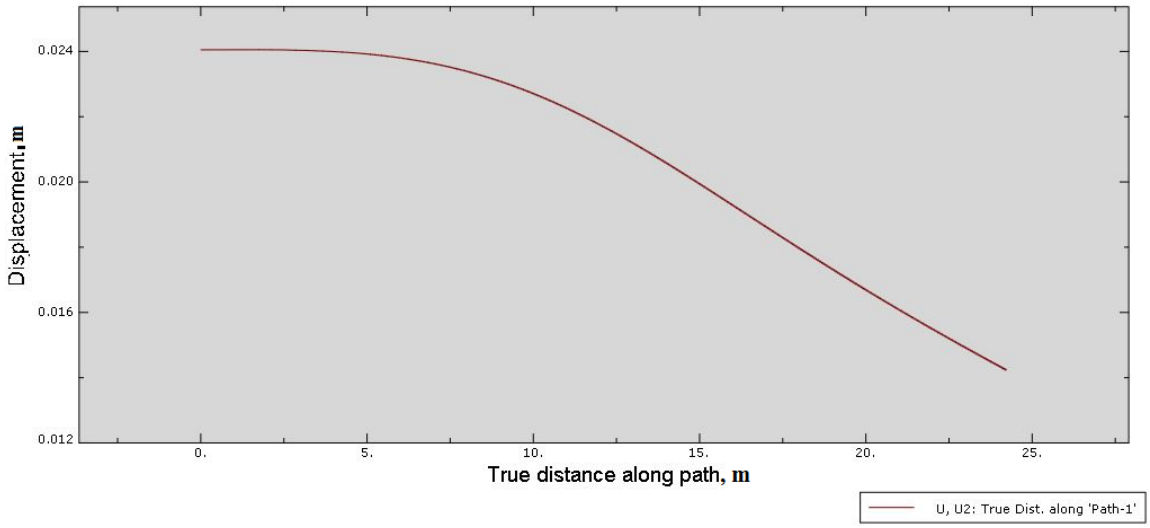

Figure 4.5 Rail settlement along the length of the track (for speed of 200km/hr)

In the above figure to see the deformation on the rail structure especially at transition section closer I just considered only the transition length (approximately 25m length). Beyond the 25m there is the slab structure. So as we can see briefly there is abrupt deformation at the transition zone.

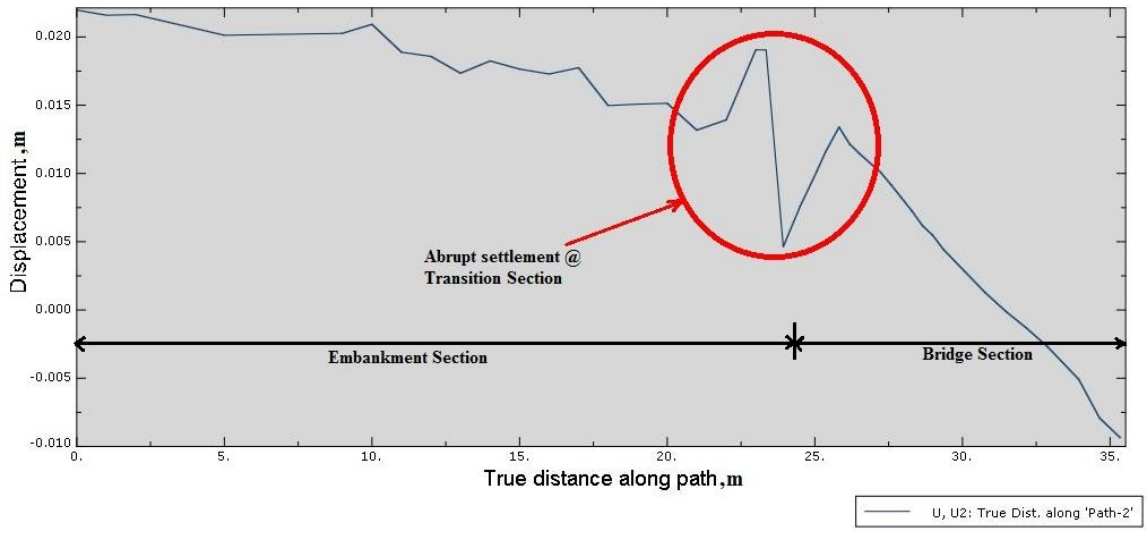

Figure 4.6 settlement along the length of the track (below the rail)

In the above figure it is shown that the embankment region (left side) show more settlement than slab region (right side) and exactly in the connection between the two regions there is abrupt settlement which ultimately create higher stress on the rail structure.

N.B. on the right side the slab deformation shows negative settlement and it is because on that side of the model the slab was not restrained against vertical movement, but practically as there will be abutment support the deflection will be constant as that of left side abutment support.

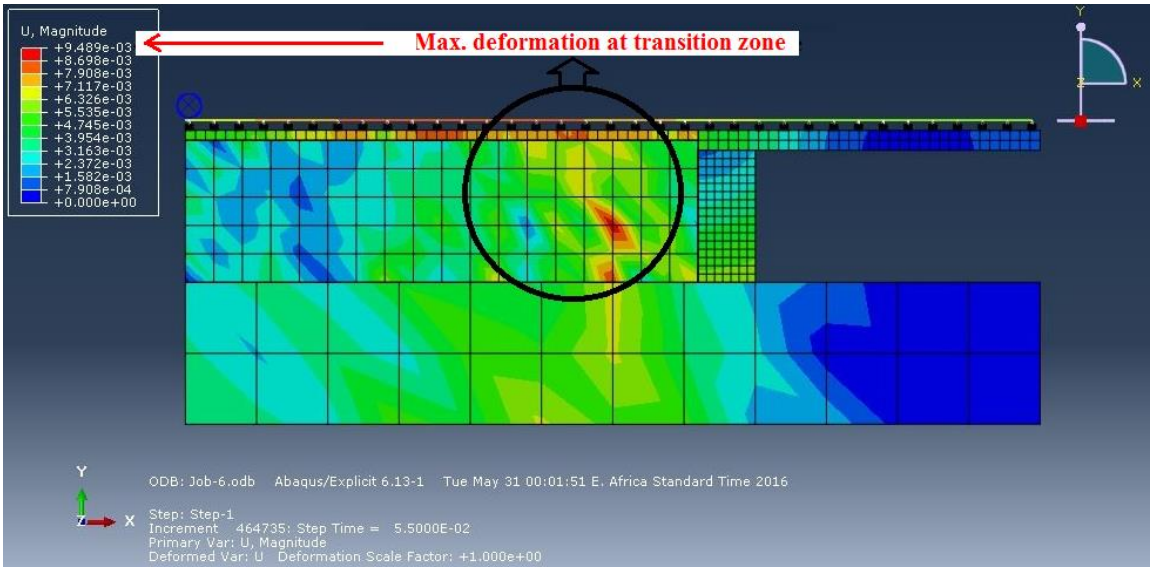

Figure 4.7 Deformation at transition zone (for forward speed of 200km/hr) (m)

According to (Singh, 2003) At typical freight train operation speeds even without any initial differential track settlement, a large track stiffness change alone would lead to marginally higher 6% dynamic load variation between the approach and bridge sections**.** More importantly, it would lead to redistribution of rail-tie interaction forces over the approach and bridge areas, i.e., much higher rail-tie interaction forces on the bridge than in the approach. If a differential settlement due to geometry degradation is also present, then both dynamic wheel loads and rail-tie interaction forces will become very significant in the approach and bridge areas.

Therefore, from the above discussions, the maximum stress obtained in this research was 126.7MPa (i.e. at transition location where abrupt support stiffness can be visualized) and on a normal embankment section stress varies between 115-120MPa, so if we take

the stress in a normal track (without sudden support stiffness variation) to be 120MPa, we can calculate the percent increment of stresses of the two locations as follows:

$$\text{Percent Increment of Stress, PIS (\%)} = \frac{126.7\ MPa - 120MPa}{120MPa} = 0.056 = 5.6\%$$

So the value of the stress increment is 5.6% (i.e. because of the abrupt settlement at the transition location the stress coming on the rail will be amplified by 5.6%)

4.3. Crack Analysis in FRANC 3D

In the third chapter, the dynamic impact factor ∅ (dimensionless impact factor) was considered to convert the vertical static wheel load (Ps) to design load (P^D). But in transition sections the design wheel load will cause additional amplified stress on the rail due to the track modulus (track support stiffness) difference. As explained above when the train moves from the bridge to the embankment section the stress is increased by 5.6% by the sudden settlement at this transition zone.

Therefore, the stress on the rail caused by the design wheel load after the increment will be:

Stress on the Rail = the hertz stress contact pressure*(1+ Percent Increment of Stress)

$$= Po * (1+PIS) = 1.056*1650.5MPa = 1742.93MPa$$

4.3.1. Three Dimensional Rail Model Results

After performing the simulation in ABAQUS by applying the amplified stress (1742.93MPa) expected at transition zone the results are obtained in the form of stress distributions.

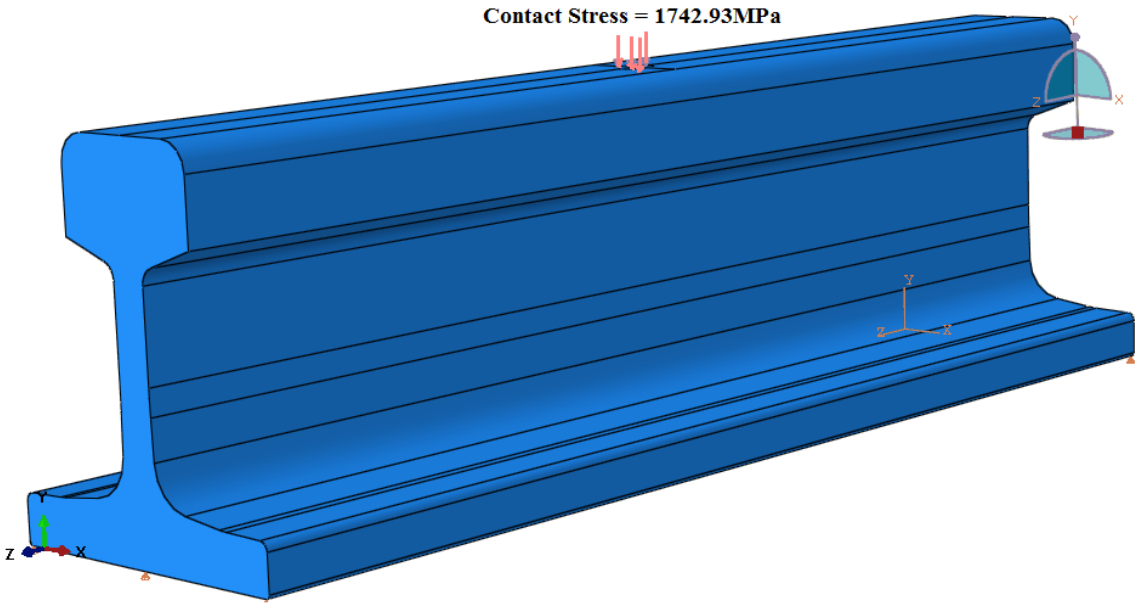

Figure 4.8 Amplified Contact Stress on the Elliptical Contact Patch

The results obtained from ABAQUS are described as follows;

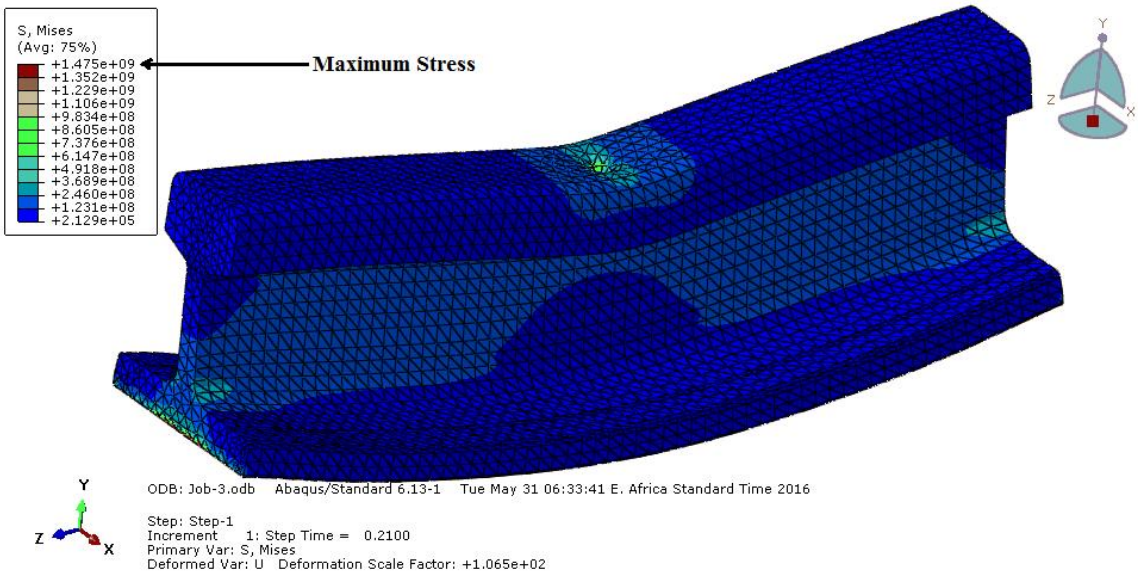

Figure 4.9 Von misses stress distribution for the rail (Pa)

Therefore, from the stress distribution results obtained in the form of Von-Misses stresses and the maximum value is found to be 1475MPa.

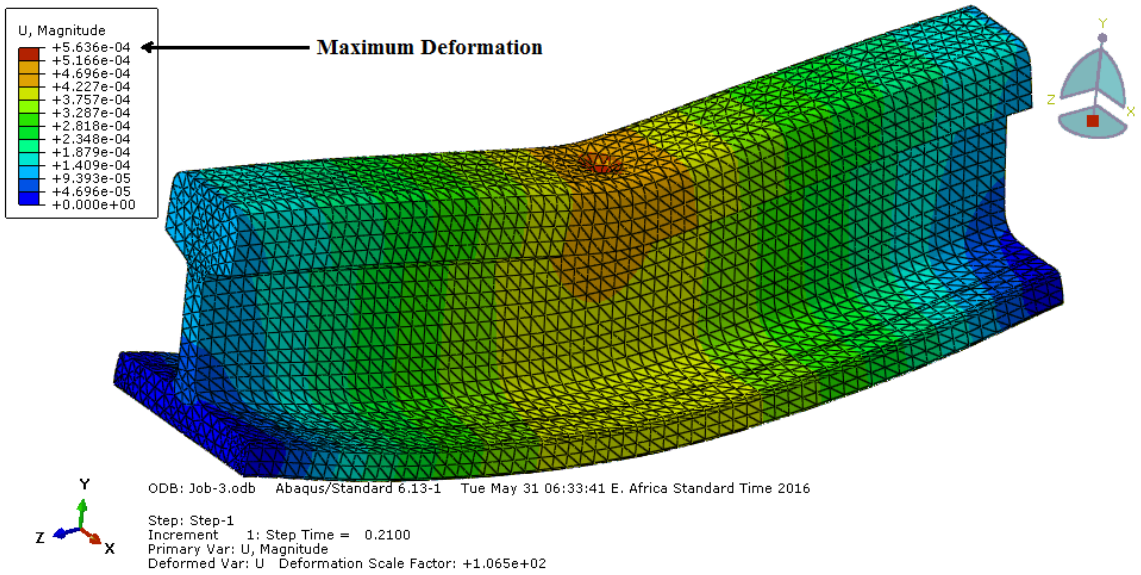

Figure 4.10 Spatial deformations at the rail nodes (m)

4.3.2. Determination of Critical Crack Size on the Rail

The propagation of a crack is driven by the stress field that develops ahead of the crack tip. In fracture mechanics, the stress and strain fields can be characterized by parameters such as the stress intensity factor, K, under elastic conditions. The stress intensity factor (K) is used in fracture mechanics to predict stress intensity near the tip of a crack caused by a remote load or residual stresses.

In general, stress-intensity factor depends on the stress induced on a structure, the crack size and the geometry of the crack. Such parameters describe the mechanics of the crack in terms that include the applied load and the length of the crack.

It is noted that the use of stress intensity factor implies that the Paris and Erdogan's equation only applies to essentially elastic solution, so that the factor provides a reasonable description of a crack tip stress field for a distance up to 0.1a from the crack tip. At any point along the boundary of the elliptical crack, the mode 1 stress intensity factor can be written as:

$$K = \frac{\sigma\sqrt{\pi a}}{\varphi}\sqrt[4]{\left(\frac{a^2}{c^2}Cos^2\theta + Sin^2\theta\right)} \quad \text{----------4.2}$$

Where, σ is the far field stress, a is the crack size, Θ is the angle that defines any point around the perimeter of the elliptical crack, and φ is the elliptical integral of the second kind, given by:

$$\varphi = \int_0^{\frac{\pi}{2}} \sqrt{\left(1 - (1 - (\frac{a}{c})^2 \sin\theta\right) d\theta} \text{----------4.3}$$

Where, a is crack depth and c is crack length.

An empirical expression that can describe the quantity φ of above equation for different crack depth to crack length aspect ratios, a/c, is given by Pook, 2000;

$\varphi^2 = 1 + 1.464 \frac{a^{1.65}}{c^{1.65}}$ for a/c ≤ 1----------4.4

$\varphi^2 = 1 + 1.464 \frac{c^{1.65}}{a^{1.65}}$ for a/c > 1----------4.5

When the crack is circular, where the aspect ratio a/c=1, φ = 2.464, the value of stress intensity factor around the crack front is a constant. From above equation, the stress intensity factor corresponding to an elliptical crack with aspect ratio a/c≤1) can be written as:

$$Ki = \frac{\sigma\sqrt{\pi a}}{\varphi} = 0.806\sigma\sqrt{a} \text{ ----------4.6}$$

Where the quantity φ = 2.464.

The finite element method (FRANC3D) was used to calculate the stress intensity factor due to the complexity of the rail geometry.

4.3.2.1. Analysis Procedures used in FRANC3D

FRANC3D (Fracture Analysis Code 3 Dimensional) is a highly interactive program for the simulation of crack growth and it is considered to be a significant step in the development of discrete fracture analysis because of its modular software design and topological data structure. The procedures followed in FRANC3D are discussed as follows:

First, we need to import results from ABAQUS for the development of a FE model for stress intensity factor determination as well as crack propagation analysis. A number of files will be created automatically as ABAQUS runs including an .inp file with the job name as the prefix. This is the file that will be read by FRANC3D.

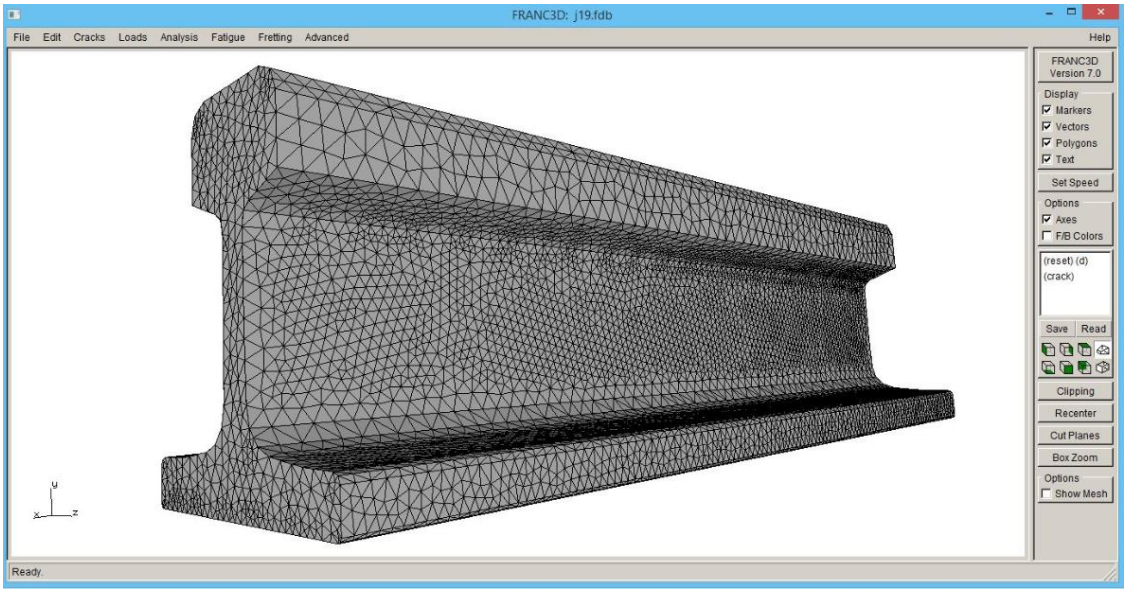

Figure 4.11 ABAQUS model imported to FRANC3D

Next**,** we define a new flaw (crack) wizard with a circular crack of radius=0.001, centered on the rail bottom face, and parallel to the xz-plane. The initial crack size, ai is assumed to be 10%Base Area (BA) (equals to 0.009m^2 for T60 rail), which roughly corresponds to the smallest defect size that non-destructive testing equipment can detect. Because according to results of different researches growth of elliptical base defect for rails range from 10 to 50%BA (DavidY. Jeong, 2012).

Once the crack geometry has been inserted to the rail model geometry (surface) and then volume meshing occurs. The final mesh is smoothed to improve the element quality.

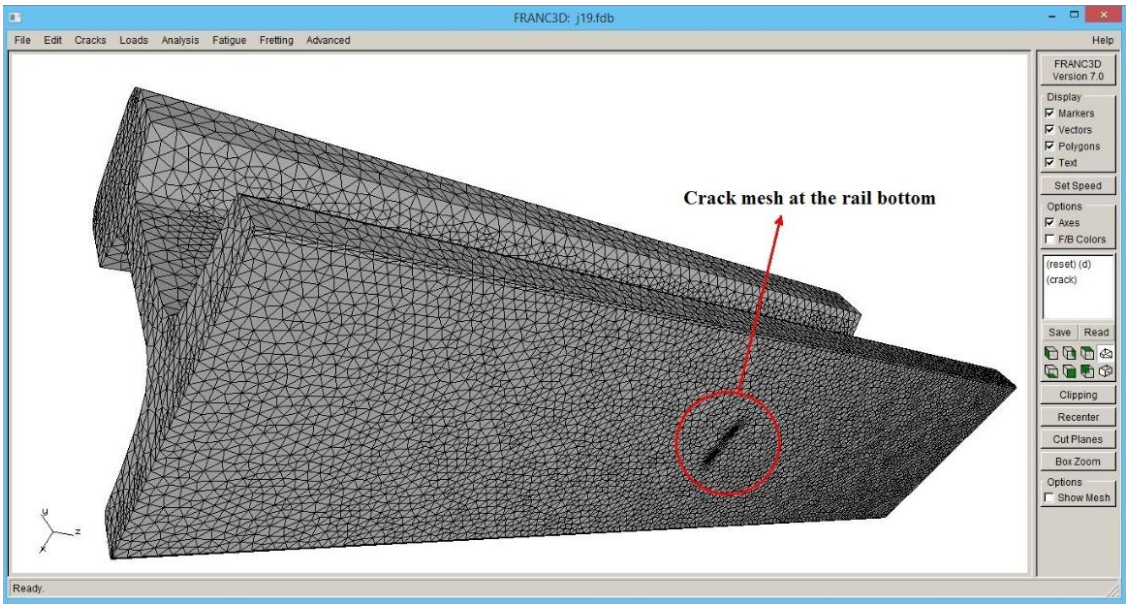

Figure 4.12 Meshed rail model with crack at rail bottom

After the crack is inserted and meshed then static crack analysis follows. Static crack analysis is a static (single step, no crack growth) deformation analysis. This analysis is wanted to compute stress-intensity factors for this crack without performing any crack growth.

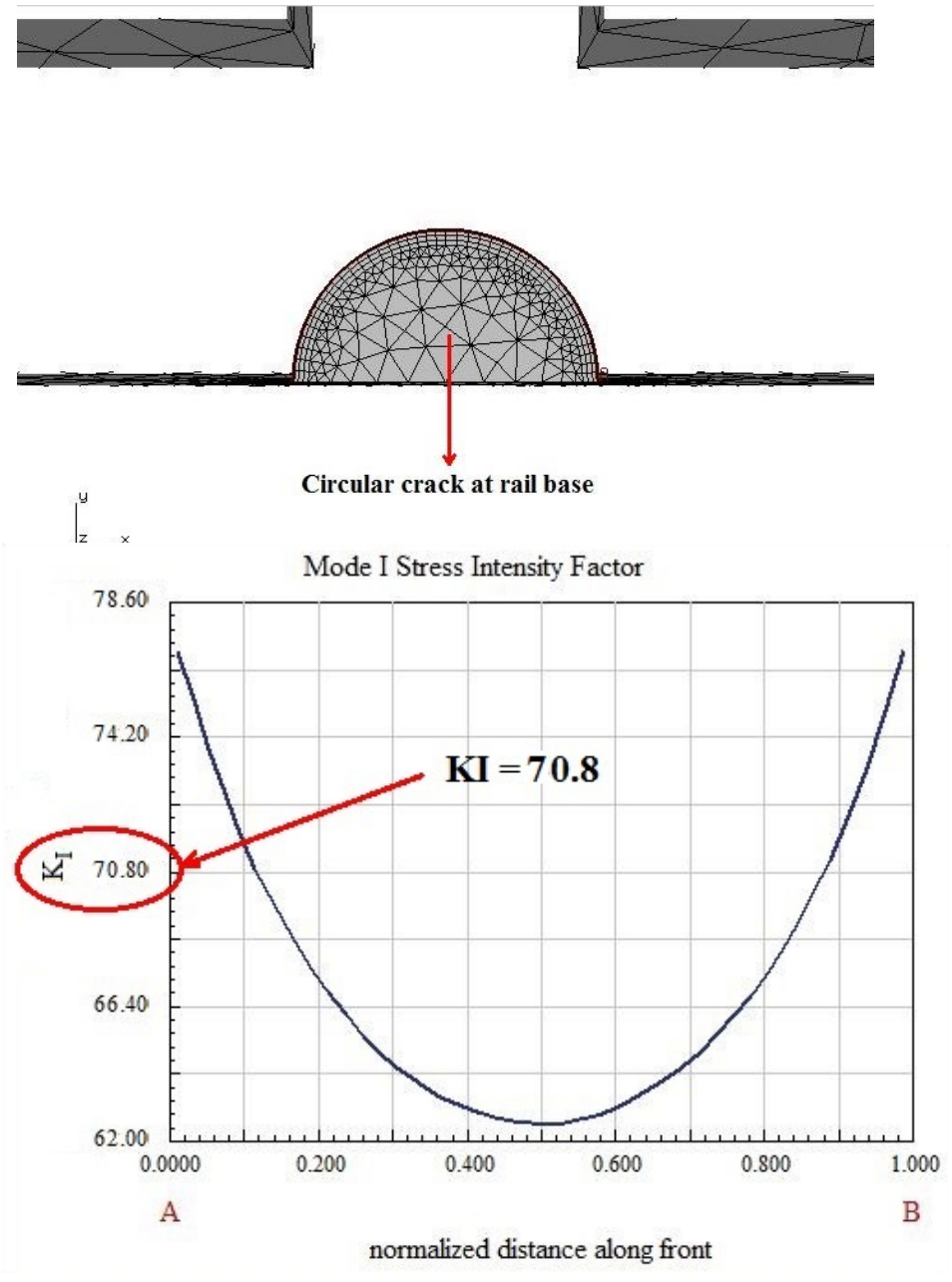

Figure 4.13 Mode I (KI) stress intensity factor with respect to normalized distance along crack front in FRANC3D

And now we need to determine the crack size at bottom and top of the rail. In materials science, a fracture toughness KIC is a property which describes the ability of a material

containing a crack to resist fracture. The subscript I denotes mode I crack opening under a normal tensile stress perpendicular to the crack. Fracture toughness is a quantitative way of expressing the resistance of a material to brittle fracture when a crack is present. It is independent of the size and geometry of the cracked body under certain conditions. The materials with higher values of fracture toughness are more likely to undergo a ductile fracture; however, the materials with low value fracture toughness usually undergo a brittle fracture (Anderson, T.M., 1999). The largest crack a structure can sustain under specific strength requirements can be predicted through this critical value of the SIF where the crack propagation becomes unstable.

The national standards of the people's republic of China manual recommend the following for the fracture toughness of rail steel: 'The minimum single value of fracture toughness KIC of rails shall be 26MPa√m and the minimum mean value shall be 29MPa√m'. The FRANC3D software mode 1 stress intensity factor value obtained before is 50.8MPa√m and it is above the minimal value.

So, the critical crack size at the base and head of the T60 rail steel can be calculated by setting the fracture criterion is: KI=KIC, as follows:

CASE 1: At rail base: $a_c = \frac{1}{\pi}\left(\frac{K\varphi}{1.12\sigma c}\right)^2 = \frac{1}{\pi}\left(\frac{70.8*2.464}{1.12*1475}\right)^2 = 3.5mm$

CASE 2: At the rail head: $a_c = \frac{1}{\pi}\left(\frac{K\varphi}{1.12\sigma c}\right)^2 = \frac{1}{\pi}\left(\frac{70.8*2.464}{1.12*1742.93}\right)^2 = 2.5mm$

Table 4.2 Crack length vs. number of cycles for rail base

Crack length (ao) (mm)	**Crack length (a) (mm)**	**ΔN (Cycles)**	**N (Cycles)**
0.001		1883.24	1883.24
0.001	0.0015	1327.14	3210.38
0.0015	0.002	1211.63	4422.01
0.002	0.0025	1111.09	5533.10
0.0025	0.003	1028.80	6561.90
0.003	0.0035	950.87	**7512.77**

Table 4.3 Crack length vs. number of cycles for rail head

Crack length (ao) (mm)	Crack length (a) (mm)	ΔN (Cycles)	N (Cycles)
0.001		1141.55	1141.55
0.001	0.0015	803.22	1944.77
0.0015	0.002	735.29	2680.06
0.002	0.0025	661.16	3341.22

According to the predicted traffic volume in the feasibility study of Some National Railway Network of Ethiopia, the forecasted number of trains varies from section to section. Assuming the annual traffic density for the National Railway Network of Ethiopia to be 22.67MGT (Million Gross Tones) the number of trains per day can be determined from the U.S. Department of Transportation (U.S. DOT) Volpe Transportation Systems Center empirical formula which is as a function of annual traffic density as follows:

X (No. Of trains per day) = T/(0.006312*365) = 9.8 ≈ 10.

Finally, the fatigue life of rail as a function of MGT (Million Gross Tones) is obtained as follows: Assume one train passes a certain track section two times per day. So, the total number of cycles per year for loaded standard vehicle with four axles or eight wheels is

8*(10*365) =29,200 cycles/year.

Then if the total number of cycles per year is 29,200 Cycles for 22.67 MGT annual traffic density by simple mathematics we can obtain the traffic density for 7,512.77 number of cycles which is the maximum No. Of cycles from rail base and head to be 5.83MGT (Million Gross Tones).

4.4.The Frequency of Rail Inspection and Maintenance

The frequency of rail inspection tends to vary from one railroad to another, yet it is usually based on either time or traffic tonnage. Railroad companies have evolved their rail inspection schedules empirically, based on long field experience. Rail defect management refers to the development and implementation of strategies to control the risk of rail failure. Rail defect inspection should be scheduled such that the occurrence of broken rails is minimized. The primary method to control the risk is a rail inspection through nondestructive evaluation and is a replacement of rails based on the remedial action plan as well as evaluation results.

From the previous crack analysis, with the assumption of 22.67MGT (Million Gross Tones) annual traffic density the fatigue life of rail based on the maximum critical number of cycles for rail base is taken as 5.83MGT (Million Gross Tones). Therefore, the frequency of rail inspection required will be:

Frequency of rail inspection per year $= \frac{5.83MGT}{22.67MGT} = 0.25$

I.e. number of rail inspection per year should be four or (in every three months the rail needs inspection).

Table 4.4 Recommended rail defect inspection frequencies

Annual Day-to-Day Traffic (Car Movements)	**Inspection Frequency**
1 million gross tons (MGT) or more (greater than 7,200 car movements per year).	3 years or 3 MGT, whichever is less
0.5 to 0.99 MGT (3,600 to 7,200 car movements per year).	5 years or 5 MGT, whichever is less
Less than 0.5 MGT (less than 3,600 car movements per year).	6 years or after a rail break

Source: Rail road track standards by US Departments of the Army and the Air Force

According to Rail road track standards by US Departments of the Army and the Air Force the recommendations are listed above. Therefore, for the value we get at the transition section i.e. 5.83MGT or 7,512.77 Cycles as it exceeds 1 million gross tones (MGT) or 7200 car movements per year the recommended rail defect inspection frequency is 3 years or 3 MGT whichever is less.

Generally, from all the above recommendations we choose the one which give us the minimum period of inspection interval. Therefor it is recommended to inspect the rail every three month to increase the service life of the rail and to minimize expected accidents.

Repeated from table 2.2 (Remedial Action Table in JR East)

Types of Defects	Criteria [mm]	Remedial action
Vertical split head	$5 \leq a < 15$	Marking for check
	$15 \leq a < 30$	Apply bolted joint bar and plan to replace
	$30 \leq a$	Replace immediately
Broken Base	$a < 3$	Apply bolted joint bar and plan to replace
	$3 \leq a$	Replace immediately

The crack at the rail base was obtained to be 3.5mm, so according to the remedial actions recommended by the Japanese Railway company, since a > 3mm the rail is better to be replaced.

Repeated from table 2.3 (Remedial action Table in DOT)

Types of Defects	Criteria [mm]	Remedial action
Vertical split head	$2.54 \leq a < 5.08$	Limit operating speed over defective rail to 48 [km/h]
		Inspect the rail 30 days after it is determined to continue the track in use
Broken Base	$2.54 \leq a < 15.24$	Apply joint bars bolted within 10 days after it is determined to continue the track in use
		After applying the jointed bars, limit operating speed to 80 [km/h]

According to US Department of Transportation (DOT), since the crack is between 2.54 and 15.24mm it is recommended to apply jointed bars bolted within 10 days after it is determined to continue the track in use. Then after applying the joint bars, limit operating speed to 80 km/h.

Based on the present rail crack value and the recommended remedial action plans the rail should be replaced when rail base crack of more than 3.5mm and head crack of more than 2.5mm is observed or apply jointed bars bolted within 10 days after it is determined to continue the track in use. Then after applying the joint bars, the operating speed should be limited to 80 km/h.

5. Conclusion and Recommendation For Future Works

5.1. Conclusion

This thesis discuss about rail damage that occurs at transition section which is known to be a location where sudden change in track modulus (track support stiffness) difference is visualized. So because of this sudden support stiffness variation the rail will be subjected to abrupt stress variation which is amplified when compared to normal track sections where there is no abrupt track modulus variation.

According to the results we get from this paper when we compare normal track sections with transition sections the amplified stress may increase up to 5.6% which ultimately fasten the rate of the rail damage on these transition sections. In order to minimize the occurrence of broken rails, rail defect inspection should be scheduled such that the risk of rail failures and the rate of derailment happening will be minimized. The primary method to control the risk is a rail inspection through nondestructive evaluation and is a replacement of rails based on the remedial action plan as well as evaluation results.

Therefore, based on the paper outputs with the above stress increment value the rail cracks up to 3.5mm at the base and 2.5mm at the head, then the main conclusions obtained from the research are:

- ✓ Inspect the rail in every three months (four times in a year) to extend the rail life, reduce the rail maintenance work and its cost.
- ✓ Based on the present rail crack value and the recommended remedial action plans the rail should be replaced when rail base crack of more than 3.5mm and head crack of more than 2.5mm is observed, or
- ✓ Apply jointed bars bolted within 10 days after it is determined to continue the track in use. Then after applying the joint bars, the operating speed should be limited to 80 km/h.

Generally, the probability of derailment happening is small because from in depth experiments the rail is able to pass trains as long as the gap due to the break is up to 70mm. But as cracks can propagate with increased number of cycles the rail should be maintained frequently.

5.2. Recommendation for Future Works

This thesis focuses on the effect of track modulus (track supporting materials stiffness) difference on rail damage and the model considered to represent the transition section was a two dimensional finite element model. However, several issues need further development and refinement to get more accurate output which approach the real world scenario. Some of the recommendations for future works include:

- Considering a three dimensional (3D) finite element model with an increased length of the transition zone to get more accurate result and to better simulate the research problem with the real (practical) problem in the service life of the track structure.
- Considering other factors that affect track modulus, like environmental factors, sleeper suspension due to ballast flying, imperfection of rail joining and soon. For instance, on the rainy season the effect of water should be given higher attention because it lubricate the rail and highly contribute to the rail crack growth in addition to its effect on the subgrade by affecting its bearing capacity which intern contribute to track settlement.
- Further extend this work by doing Life Cycle Cost (LCC) analysis for the rail found on this transition section which include optimal repair and maintenance schedule.

REFERENCES

American Railway Engineering and Maintenance of Way Association (AREMA),

Andersson E, Berg M and Stichel S, (2007). Rail Vehicle Dynamics. Text book, Division of Rail Vehicles, Department of Aeronautical and Vehicle Engineering, Royal Institute of Technology (KTH), Stockholm.

Australian Rail Track Co., (2006). "Rail Defects Handbook," Engineering Practices Manual.

Australian Transport Safety Bureau, (2012). "Australian Rail Safety Occurrence Data from 1 July 2012 to 30 June 2012".

Bower, A.F. and Johnson, K.L. (1991). Plastic flow and shakedown of the rail surface in repeated wheel-rail contact Wear.

Cannon, D.F., Edel, K.O., Grassie, S.L. and Sawley, K. (2003). Rail defects: an overview. Fatigue & Fracture of Engineering Materials & Structures.

Department of transportation (2007), Bridge approaches and track stiffness, U.S. Federal Railroad Administration.

Diamond, S. and Wolf, E. (2002). Transportation for the 21st Century. Track Guide Top-of-Rail Lubrication System, Report from Department of Energy, USA.

Cheng Chen (2003). Discrete Element Modeling of Geogrid-Reinforced Railway Ballast and Track Transition zones.

David Y. Jeong, A. Benjamin Perlman, (2011). Estimating track capacity based on rail stresses and metal fatigue, USA.

Dingqing Li and David Davis (2005), Transition of Railroad Bridge Approaches, USA

Drucker, D. C., & Prager, W. (1952). Soil Mechanics and Plastic Analysis or Limit Design.

Eisenmann, J (1970) Stress Distribution in Permanent Way due to Heavy Axle Loads and High Speed, Berlin.

Esveld, C. (2001). Modern Railway Track. Delft: MRT-Productions, 2nd ed., Germany.

G. Zi, S. Y. Jang, S.C. Yang, H.S. Lee, E. Kim, (2012). "Investigation of a concrete railway sleeper," Engineering Failure Analysis.

H. Sundquist, Byggande, (2000). Drift och Underhåll av Järnvägsbanor, TRITA-BKN, Rapport 57, KTH, Stockholm (Compendium in Swedish).

Iwnicki S: A handbook of railway vehicle dynamics, CRC Press, ISBN 0849333210, London 2006.

IHHA (2001) Guidelines to Best Practice For Heavy Haul Railway Operations: Wheel and Rail Interface Issues. International Heavy Haul Association, Virginia, USA.

Ivo Seara, (2007), Performance assesment solutions for transition zones embankment-bridge railways trough numerical simulation 3d, V. N. Famalicão, Portugal

J. Maes, H. Sol, and P. Guillaume, (2006). "Measurements of the dynamic railpad properties," journal of sound and vibration.

Larsson, D. (2004). A Study of the Track Degradation Process Related to Changes in Railway Traffic. Licentiate Thesis. Division of Operation and Maintenance Engineering,

Lichtberger, B. (2005). Track Compendium. Eurail press, 1st ed., Hamburg, Germany.

P. Paris and F.Erdogan (1963), "A Critical Analysis of Crack Propagation Low," Journal of Basic Engineering, ASME, Vol.85, No.4

Xiaoi Shi (2009), Prediction of Permanent Deformation in Railway Track.

K. Tzanakakis, (1992). Railway Track and Its Long Term Behavior: A Handbook for Railway Track of High Quality.

Redden, J. W., Selig, E. T., and Zaremsbki, A. M. (2002). "Stiff track modulus considerations." Railw. Track Struct, February, 25–30.

Rippeth, D., Kalousek, J. and Simmons J. (1996). A case study of the effect of lubrication and profile grinding on low rail roll-over derailments.

Selig, E. T., and Li, D. (1994). "Track modulus: Its meaning and factors influencing it." Transportation Research Board, Washington, D.C., 17–25.

Selig, E. T., and Waters, J. (1994). Track geotechnology and substructure management, Thomas Telford, London.

T. Dahlberg, (2010). "Railway track stiffness variations-consequences and countermeasures," International Journal of Civil Engineering, vol.8, no.1, pp.1–12.

Timoshenko, S., Langer, B., (1932) Stress in Railroad Tracks, ASTM

The national standards of the people's republic of China manual (GB)

U. Zerbst, (2009). "Introduction to the damage tolerance behavior of railway rails- a review," Engineering Fracture Mechanics.

Van Den Bosch, R.A. (2002). Rail grinding strategies on Netherlands railways. Rail Engineering International.

Wilson, L. (2006). Optimization of Rail/Wheel Lubrication. PhD Thesis, Queensland University of Technology, Brisbane, Australia.

W. M. Zhai, (2004). "Modelling and experiment of railway ballast vibrations," journal of sound and vibration.

X. Lei and L. Mao, (2004). "Dynamic response analyses of vehicle and track coupled system on track transition of conventional high speed railway," Journal of Sound and Vibration,.

Y. S. Kang, S.C. Yang, H.S. Lee, E. Kim, (2006). A Study of Track and Train Dynamic Behavior of Transition Zone between Concrete Slab Track and Ballasted Track, Korea Railroad Research Institute, Uiwang, South Korea.

Zarembski, A.M., Grissom, G.T. and Lees Jr., H.M. (2005). Assessing the risk of track buckling: to reduce the risk of track buckles. Railway Track and Structures.

APPENDIX

Table A-1 Calculated data of rail

Rail style (kg/m)	Section area (cm^2)	Center of gravity from bottom of rail (cm)	Center of gravity from ends of rail (cm)	Moment inertia of horizontal axis (cm^4)	Moment inertia of vertical axis (cm^4)	Cross-section coefficient of bottom (cm^3)	Cross-section coefficient of top (cm^3)	Cross-section coefficient of bottom side edge (cm^3)
38	49.5	6.67	6.73	1204.4	209	180.6	178.9	36.7
43	57.0	6.90	7.10	1489.0	260	217.3	208.3	45
50	65.8	7.10	8.10	2037.0	377	287.2	251.3	57.1
60	77.45	8.12	9.48	3217	524	369.0	339.4	69.9
75	95.037	8.82	10.38	4489	665	509	432	89

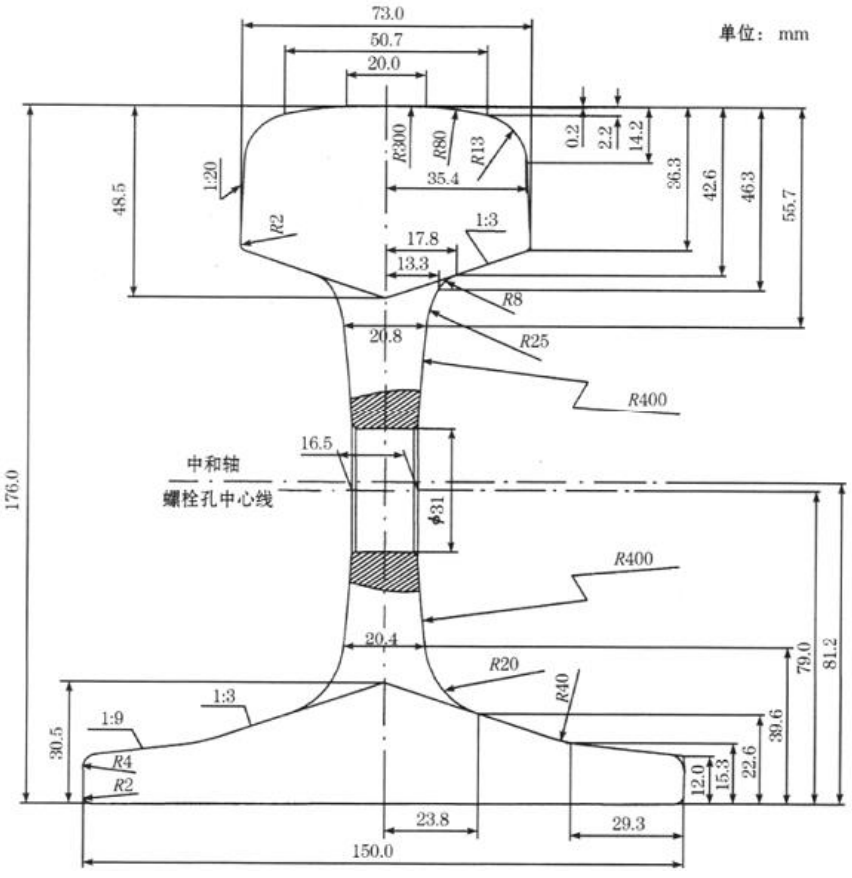

Figure A-1 Cross-section for 60kg/m rail profile

Table A-2 Hertz coefficients

θ (deg)	**m**	**n**	**θ (deg)**	**m**	**n**	**θ (deg)**	**m**	**n**
0.5	61.4	0.1018	10	6.604	0.3112	60	1.486	0.717
1	36.89	0.1314	20	3.813	0.4125	65	1.378	0.759
1.5	27.48	0.1522	30	2.731	0.493	70	1.284	0.802
2	22.26	0.1691	35	2.397	0.530	75	1.202	0.846
3	16.5	0.1964	40	2.136	0.567	80	1.128	0.893
4	13.31	0.2188	45	1.926	0.604	85	1.061	0.944
6	9.79	0.2552	50	1.754	0.641	90	1.0	1.0
8	7.86	0.285	55	1.611	0.678			

Source: railroad vehicles dynamics: a computational approach (2008)

- Sample Calculation for values obtained in Table 4.2 Crack length vs. number of cycles for rail base:

$$\Delta K = 0.806\sigma c\sqrt{a} = 0.806 * 1475\sqrt{0.001} = 37.59$$

$$\frac{da}{dN} = C(\Delta K)^m = 1 * 10\text{e} - 11(37.59)^3 = 5.31*10^{-7}$$

$$dN = \frac{0.001}{5.31 * 10e - 7} = 1{,}883.24$$